https://doi.org/10.1016/j.trc.2023.104054

Condition-Based Pavement Management Systems Accounting for Model Uncertainty and Facility Heterogeneity with Belief Updates

Le Zhang[a], Weihua Gu[b†], and Young-Ji Byon[c], Jinwoo Lee[d*]

a: School of Economics and Management, Nanjing University of Science and Technology, Nanjing 210094, China, Email: le.zhang@njust.edu.cn, ORCID: 0000-0003-2541-7956

b: Department of Electrical Engineering, The Hong Kong Polytechnic University, Hung Hom, Kowloon, Hong Kong, China, Email: weihua.gu@polyu.edu.hk, ORCID: 0000-0003-3848-4840

c: Department of Civil Infrastructure and Environmental Engineering, Khalifa University of Science and Technology, Abu Dhabi, UAE, Email: youngji.byon@ku.ac.ae, ORCID: 0000-0003-1209-1803

d: The Cho Chun Shik Graduate School of Green Transportation, Korea Advanced Institute of Science and Technology, Daejeon, Republic of Korea, Email: jinwoo@kaist.ac.kr, ORCID: 0000-0002-6692-9715

*: Corresponding Author

†: Co-corresponding Author

ABSTRACT

Due to the tighter budget for pavement management, schedules of inspection activities should be jointly optimized with the maintenance and reconstruction (M&R) plans for pavement systems. Conducting inspections every year is unnecessary and will decrease the budget for M&R activities, while infrequent inspections may lead to suboptimal M&R planning due to the lack of accurate information. This paper presents a methodology for jointly optimizing the inspection scheduling and M&R planning for pavement systems, considering model uncertainty and facility-specific heterogeneity. The problem is defined as a Partially Observable Markov Decision Process (POMDP) model, accounting for the tradeoff between the information value and inspection costs. Moreover, a statistical learning method is used to update the prediction of pavement conditions using the collected inspection data. This "belief update" process can gradually reduce the model uncertainty as the dataset size increases. We demonstrate the proposed stochastic optimization framework through a numerical example with a system of fifty heterogenous pavement facilities under a combined budget for inspection and M&R activities. Several managerial insights and implications are discussed. For example, the optimal inspection frequencies are less sensitive to the budget; and the agency should perform fewer reconstructions and more rehabilitations when the budget is limited.

Keywords: pavement management systems; uncertainty; heterogeneity; inspection; M&R; POMDP; belief update.

1. INTRODUCTION

Pavement systems play a vital role in national economies and people's daily lives. The healthy operating condition of pavement systems is essential for satisfying the daily transportation demand and ensuring traffic safety and comfort (Levenberg et al., 2016; Mack et al., 2018; Richmond et al., 2018). For example, the United States alone has over 4 million miles of pavement serving 3 trillion vehicle-miles per year (ASCE, 2017). However, in recent decades, the rapidly growing vehicle demand has accelerated the deterioration and aging of pavements. On the other hand, the government budgets for pavement management rise at consistently lower rates than needed (ASCE, 2017). As a result, the poor pavement conditions induce lower vehicle fuel efficiencies and more damage, including tire wear and suspension breakdowns. The ensuing user cost is huge (Islam and Buttlar, 2012). This dilemma makes efficient management of pavement systems under a limited budget increasingly important.

Optimal pavement maintenance and reconstruction (M&R) strategies have been widely studied under deterministic scenarios where the future pavement states in response to deterioration and M&R activities are assumed to be predictable (Chu and Chen, 2012; Lee and Madanat, 2015; Qiao et al., 2017; Zhang et al., 2017; Chu and Huang, 2018). Unfortunately, the real pavement deterioration process cannot be accurately predicted due to multiple stochastic factors, including epistemic uncertainty, utilization levels, and environmental conditions (Madanat, 1993; Durango-Cohen, 2004; Swei et al., 2018). Erroneous predictions would lead to inappropriate M&R policies and higher total lifecycle costs for the pavement system. Thus, it is imperative to model the uncertainties and incorporate inspection scheduling into the pavement management problem.

This paper will model the optimal inspection and M&R strategies for pavement systems considering inherent uncertainties in the deterioration process. Inspections will be included in the decision process to provide accurate data for: (i) optimal M&R planning and (ii) updating the management agency's knowledge about the uncertainties. The schedule of inspections is jointly optimized to ensure more effective utilization of the limited budget.

We next review the literature in the realm of pavement management optimization.

2. LITERATURE REVIEW

Research on pavement management problems has a long history, with some earliest studies dated 40 years ago (Friesz and Fernandez, 1979; Fernandez and Friesz, 1981). A variety of optimization

models in this realm have thenceforth been developed. They can be characterized by the deterioration process (memoryless or history-dependent; deterministic or stochastic), the number of treatment types (single or multiple), and whether the time or facility states are discretized. To stay focused, we next review the models and techniques considering stochastic deterioration processes.

To capture the uncertainty in pavement deterioration, pavement management models usually rely on stochastic control and optimum sequential decisions. The most basic form is the Markov Decision Process (MDP) framework (Thompson et al., 1998; Durango-Cohen, 2004). However, a fundamental assumption of MDP is that inspections can always reveal the true system state with certainty, i.e., perfect inspections. Another limitation is that an inspection is assumed to be performed at every decision period to make M&R-related decisions. In reality, pavement inspections incur costs, and frequent inspections may further increase the financial burden of management agencies. To address these limitations, MDP is extended to Partially Observable MDP (POMDP) (Madanat, 1993; Papakonstantinou and Shinozuka, 2014a, 2014b; Memarzadeh et al., 2016; Schöbi and Chatzi, 2016; Papakonstantinou et al., 2018). In the framework of POMDP, the evolution of pavement management systems is still represented by an underlying stochastic process with Markovian dynamics. However, the decision-makers can choose actions only based on the probability distribution of actual pavement system states at any specific time, namely "system state belief." Thus, POMDP does not require the inspection intervals to be predetermined. The inspection data will be used to update the system belief and improve the accuracy of the stochastic deterioration model (Durango-Cohen and Madanat, 2002; Madanat et al., 2006; Swei et al., 2017).

For simplicity, many earlier studies assumed that the facilities in a pavement system are homogeneous. This type of pavement management problems can be solved via the so-called "top-down" approach, also known as single-dimensional MDP or POMDP. Given this premise, the optimal policy can be determined by a linear programming (LP) method. The LP-based approach provides a randomized optimal policy to accommodate budget constraints when making M&R decisions (Beutler and Ross, 1985; Ross and Varadarajan, 1989; Feinberg and Shwartz, 1996), wherein the optimal action for a facility in a given state is defined as a probability distribution over a set of candidate actions. Consequently, it cannot give any facility-specific recommendations due to the probabilistic nature of the solution. Moreover, much of the facility-specific information (e.g.,

structure, environmental factors, and construction history) is ignored in a homogeneous system. Top-down approaches are thus unrealistic and unsuitable for real-world implementations.

Hence, recent studies have focused on more realistic and facility-specific policies derived via the bottom-up approaches for a heterogeneous pavement system, known as multi-dimensional MDP or POMDP (e.g., Ouyang, 2007; Yeo et al., 2013; Donev and Hoffmann, 2020). These problems belong to a special type of resource allocation problems, termed the weakly coupled dynamic problems. Such a problem consists of multiple sub-problems that are independent of each other, except for a set of linking constraints imposed on the controls (i.e., the agency budget constraint in our model). These problems are often solved by dualizing the linking constraints through Lagrange relaxation and decomposing a large-scale system-level problem into smaller, facility-level problems, i.e., lower-dimensional MDP or POMDP (Ohlmann and Bean, 2009; Yeo et al., 2013; Torres-Machí et al., 2014; France-Mensah and O'Brien, 2018 and 2019a; Shi et al., 2020; Naseri et al., 2020). The solution time is often greatly reduced as a consequence.

The pavement management problem examined in this paper is also a weakly coupled dynamic problem in a POMDP framework where the inspection and M&R activities are subject to a limited budget constraint. Thus, the pavement's inspection schedules should be jointly optimized with the M&R decisions. A delayed inspection may cause postponed M&R activities, as the major role of inspection is to provide the information required for making optimal M&R decisions. On the other hand, frequent inspections may drain the agency's funding for M&R activities. All these interactions make it necessary to optimize inspection and M&R planning jointly under the POMDP framework. However, the size of a solution space may increase greatly due to the joint optimization of pavement inspection and M&R decisions, making the problem more complex, especially for large-scale systems. This also explains why many previous studies have assumed that inspections were performed periodically (i.e., the so-called time-based inspection scheme). To our best knowledge, only a handful of facility-level and small-sized system-level problems incorporated inspection decisions in pavement management (Madanat, 1993; Durango-Cohen and Madanat, 2002). Recently, Shon and Lee (2021) proposed a computationally efficient bottom-up solution for real-scale pavement networks. Regrettably, they also assumed a time-based inspection policy (i.e., periodic inspections independent of the current conditions of pavements). Such an inspection policy would be inferior to the optimal condition-based policy that offers variable inspection periods depending on the present facility states.

Given the above research gap, this paper will present a scalable POMDP pavement management framework for selecting condition-based optimal inspection and M&R policies under model uncertainties. The model specifies that the inspection and M&R decisions are made on the basis of the pavement condition states (i.e., the condition-based management scheme). Meanwhile, we use a statistical learning approach to improve the accuracy of the deterioration model. Our methodological contributions are briefly presented as follows:

(i) To our best knowledge, we are the first to develop a joint optimization framework of condition-based inspection and M&R activity planning for heterogeneous facilities. Compared to the conventional time-based inspection scheme, our model allows the management agency to better utilize the limited budget and reduce user costs. Moreover, we proposed an efficient approach to solve the joint optimization problem with added complexity. The approach incorporates a decomposition of the system-level problem via the Lagrange multiplier method and a tailored dynamic programming method for solving the facility-level problems.

(ii) We are also the first to incorporate belief updates of model uncertainties into the rolling-horizon-based M&R planning framework. This can further save the user cost considerably, as will be shown momentarily.

In addition, our numerical case studies unveil managerial insights that can assist agencies in planning inspection and M&R activities more effectively.

The rest of the paper is organized as follows. Section 3 presents the overall decision-making procedure. Section 4 proposes a bottom-up solution methodology. Numerical case studies are furnished in Section 5. Findings and potential extensions of the present work are discussed in Section 6.

3. DECISION PROCEDURE

We first introduce the decision procedure. Notations used in this paper are summarized in **Appendix A**. A decision-making framework for the pavement management problem is represented by selecting the optimal inspection and M&R schedules under the model uncertainty over the planning horizon. This joint optimization model guarantees that an inspection or M&R activity is made only if the expected future cost reduction offsets its cost.

Conventionally, decision-makers are more interested in available actions at present (e.g., selecting which facilities to perform inspections or M&R activities on in the current decision period) than future plans. This is because the effects of future actions are associated with higher uncertainties. However, in long-term planning, the optimal policies applied in the current period should be chosen based on the expected costs hinged on future action plans. We denote τ the current time and t the future time index (or relative time index) elapsed from the current time, both in years; $t = 0$ and $t = T$ indicate the current period and the end of the current planning horizon, respectively. Note that the planning horizon is rolling in time.

For illustration, the decision-making processes at two consecutive time points, τ and $\tau + 1$, are presented in **Figure 1**. At τ (the upper half of the figure), we aim to find the optimal inspection and M&R actions implemented at $t = 0$ (see the dark gray box). This is done by calculating and comparing the expected discounted future costs associated with each candidate action plan at $t = 0$. The expected future cost will be computed considering the optimal stochastic (i.e., mixed) inspection and M&R strategies over the rest of the current planning horizon, i.e., $t \in \{1, 2, \dots, T-1\}$ (see Arrow 1) under the available budget known at τ, B^{τ}, and the best belief of the deterioration model at τ, denoted by $\hat{d}^{\tau}$ (see Arrow 2). Deterioration model d^{τ} is estimated based on the historical data collected until τ (see Arrow 3), while the true deterioration process is denoted by d, which is unknown to us. The probability distribution of each facility's current condition is estimated based on the latest available condition, either observed by an inspection or achieved by an M&R activity (see Arrow 4).

Next, we move to time point $\tau + 1$. After the actions are applied at time τ, the decision process described above will be repeated to identify the optimal inspection and M&R action plan at $\tau + 1$, with the planning horizon rolled ahead by one unit of time (i.e., now $t = 0$ indicates time $\tau + 1$); see Arrow 5. In other words, the policies will be optimized on a period-by-period basis. This is because the estimated deterioration processes and available budget are updated at each τ in a feedback optimization framework. Other changeable factors such as costs, inspection technologies, and M&R activities are also updated in every decision period.

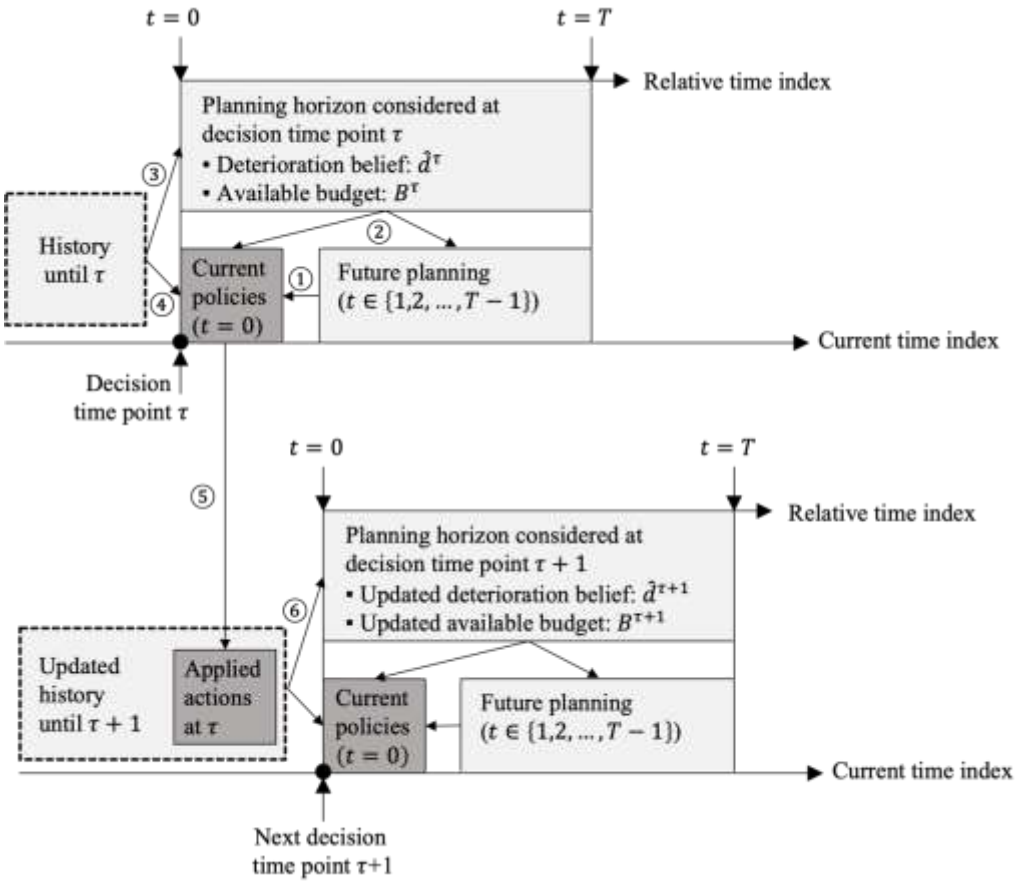

Figure 1. Graphical representation of the rolling-horizon procedure.

In detail, the pavement deterioration model $d^{\tau+1}$ will be improved by adding extra training data collected from the inspections (if any) conducted in year τ. The model's accuracy gradually improves as the inspection dataset grows during the rolling-horizon procedure. Moreover, the expected budget at $\tau + 1$, $B^{\tau+1}$, can be adjusted to reflect the actual agency expense in period τ and the perceivable political and financial situations in the future; see Arrow 6.

It is worth noting that, in the decision process of year τ, the optimal stochastic action plans are also determined for years $\tau + 1$ to $\tau + T - 1$. However, in year $\tau + 1$, with the updated deterioration model and budget, the action plan of year $\tau + 1$ must be re-optimized.

The rest of this section elaborates on the decision-making process in a typical decision period. Sections 3.1 and 3.2 present the concept of condition-based decision and the mathematical program formulation, respectively.

3.1 Condition-based decision process

At the decision-making time point τ, the system-level decision for N facilities, indexed by $n = 1, \dots, N$, is comprised of N facility-level decisions. The facility-level decision along the planning horizon T includes the current action at $t = 0$ and the future actions in periods $t = 1, \dots, T-1$. For clarity, we specify that an inspection will only be performed at the beginning of a period, immediately followed by an M&R activity. Specifically, we divide each period $t \in \{0, 1, \dots, T-1\}$ into three stages, **Stage I, II, and III**, and their beginning timestamps are denoted by t^I, t^{II}, and t^{III}, respectively, with $t^I < t^{II} < t^{III}$. The inspection and M&R activities will be decided and conducted in **Stages I** and **II**, respectively. **Stage I** at t^I is for making the decision or application of inspection to be conducted; **Stage II** at t^{II} is the time stage immediately after the decision is made or the application of inspection (if necessary) is conducted. It is also the stage to decide whether an M&R action will be taken. **Stage III** at t^{III} is the time stage after the M&R activity is performed, where the deterioration is realized.

The overall facility-level decision-making process for the current action at τ is depicted in **Figure 2** and described in detail in the rest of Section 3. Specifically, decision processes in Stages I and II are detailed in Sections 3.1.1 and 3.1.2, respectively, including the condition-based decisions in each stage and the corresponding mathematical programming function. Section 3.1.3 describes the facility condition achieved after M&R activities in Stage III. Section 3.1.4 furnishes the deterioration model.

3.1.1 Stage I: Stochastic-Condition-Based inspection

For decision-making time point τ, the initial condition of facility n at $t = 0^I$ is denoted by $S_n^\tau(0^I)$. For simplicity, the superscript "τ" is omitted hereafter in the above notation. Since the last inspection was performed before 0^I, condition $S_n(0^I)$ is a random vector associated with the true stochastic deterioration process d and the latest inspection results:

$$Prob(S_n(0^I) = s_n | d) \geq 0, \ \sum_{s_n \in \mathbb{S}_n} Prob(S_n(0^I) = s_n | d) = 1, \quad (1)$$

where $\mathbb{S}_n$ denotes the set of all possible conditions for facility n.

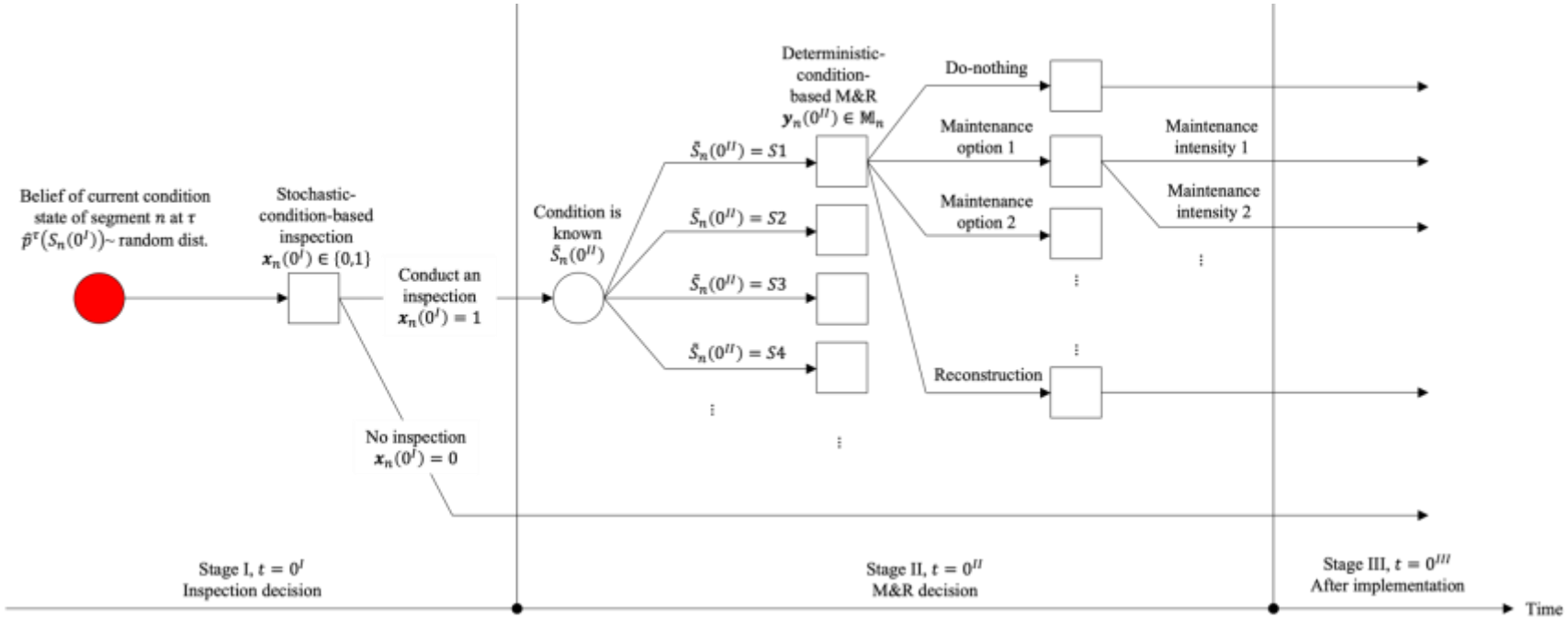

Figure 2. Decision tree for stochastic-condition-based inspection and deterministic-condition-based M&R in three stages.

The true probability distribution of the initial condition is technically unknown due to epistemic uncertainty. Instead, we do know the best available prediction, i.e., the belief of deterioration process, achieved at τ based on the data collected until τ, $\hat{d}^{\tau}$, i.e.,

$$Prob\left(\hat{S}_n(0^I) = s_n|\hat{d}^{\tau}\right) \geq 0,\ \sum_{s_n \in \mathbb{S}_n} Prob\left(\hat{S}_n(0^I) = s_n|\hat{d}^{\tau}\right) = 1, \quad (2)$$

where the estimated condition is distinguished from the truth by adding a "^". To further simplify the notation, we use $p(S_n(0^I) = s_n)$ and $\hat{p}^{\tau}(S_n(0^I) = s_n)$ instead of $Prob(S_n(0^I) = s_n|d)$ and $Prob\left(\hat{S}_n(0^I) = s_n|\hat{d}^{\tau}\right)$, respectively, to represent the probabilities and use $p\left(S_n(0^I)\right)$ and $\hat{p}^{\tau}\left(S_n(0^I)\right)$ to represent their distributions. We call $\hat{p}^{\tau}\left(S_n(0^I)\right)$ the belief of the current condition before inspection, which is the set of the probabilities of $\hat{S}_n(0^I)$.

The belief $\hat{p}^{\tau}\left(S_n(0^I)\right)$ (see the red circle in **Figure 2**) is used for the inspection decision. Thus it is termed "Stochastic-Condition-Based (SCB) Inspection." The inspection strategy is denoted by:

Stochastic-Condition-Based (SCB) Inspection at $\boldsymbol{\tau}$: $\boldsymbol{x}_n\left(0^I|\hat{p}^{\tau}\left(S_n(0^I)\right)\right)$. (3)

The binary decision variable $\boldsymbol{x}_n(0^I)$ equals 1 if an inspection will be performed at 0^I and 0 otherwise. Note that the decision variables are denoted by bold letters to distinguish them from other variables and parameters. Once an inspection is conducted, we observe an accurate current condition denoted by $\tilde{S}_n(0^{II})$. For simplicity, it is assumed that perfect and nondestructive inspections are performed, meaning that an inspection always measures the true condition without affecting the pavement, i.e.,

$$Prob\left(\tilde{S}_n(0^{II}) = s_n|S_n(0^I) = s_n, \boldsymbol{x}_n(0^I) = 1\right) = 1. \quad (4)$$

From above, $\tilde{S}_n(0^{II}) = S_n(0^I)$. Note that $Prob\left(\tilde{S}_n(0^{II}) = s_n|\hat{S}_n(0^I) = s_n, \boldsymbol{x}_n(0^I) = 1\right)$ is not always equal to one due to the difference between the measured and predicted conditions.

3.1.2 Stage II: Deterministic-Condition-Based M&R

An M&R activity to apply at $t = 0^{II}$, denoted by $\boldsymbol{y}_n(0^{II})$, can be determined based on the observed condition $\tilde{S}_n(0^{II})$ after an inspection at $t = 0^{I}$. Thus, we call it "Deterministic-Condition-Based (DCB) M&R." It requires a preceding inspection, $\boldsymbol{x}_n(0^{I}) = 1$. The DCB M&R is mathematically defined as (5) regarding the options for M&R activities, $\boldsymbol{y}_n(0^{II}) \in \mathbb{M}_n$.

Deterministic-Condition-Based (DCB) M&R at τ: $\boldsymbol{y}_n\left(0^{II} | \tilde{S}_n(0^{II}) = s_n, \boldsymbol{x}_n(0^{I}) = 1\right)$. (5)

M&R actions range from preventive maintenance to reconstruction, rendering different improvements on the pavement condition. The performance and cost of a specific M&R action usually depend on its intensity (Gu et al., 2012). Note that 'do-nothing' is also one of the actions.

The underlying assumption is that knowledge of the facility condition is required for the M&R decision-making. In other words, no M&R activity can be performed unless an inspection precedes it; i.e., $\boldsymbol{y}_n(0^{II} | \boldsymbol{x}_n(0^{I}) = 0)$ must be 'do-nothing' as described in **Figure 2**. Moreover, once the condition state is revealed as s_n by the inspection, the DCB M&R strategy, $\boldsymbol{y}_n\left(0^{II} | \tilde{S}_n(0^{II}) = s_n, \boldsymbol{x}_n(0^{I}) = 1\right)$, is applied.

3.1.3 Stage III: Condition achieved after M&R

Given the condition before the M&R decision, $\tilde{S}_n(0^{II})$, we assume the improved condition after an M&R activity, denoted by $S_n(0^{III})$, is known and deterministic. This is because the M&R procedure is controllable. For instance, a reconstruction, usually enforced by quality standards via forms of maintenance codes by DOTs, will renew the facility to its best achievable condition. Since $S_n(0^{III})$ is a deterministic function of $\tilde{S}_n(0^{II})$ and $\boldsymbol{y}_n(0^{II})$, we write $S_n(0^{III}) = f\left(\tilde{S}_n(0^{II}), \boldsymbol{y}_n(0^{II})\right)$. If $\boldsymbol{y}_n(0^{II})$ is 'do-nothing' after an inspection, $S_n(0^{III}) = \tilde{S}_n(0^{II})$. Lastly, if no inspection is carried out at $t = 0^{I}$ ($\boldsymbol{x}_n(0^{I}) = 0$), $\hat{S}_n(0^{III}) = \hat{S}_n(0^{I})$.

3.1.4 Deterioration Model

Equation (6) presents the stochastic model for the progression of pavement deterioration during Stage III:

$$\hat{p}^{\tau}\left(S_n((t+1)^{I}) = s_n | \hat{S}_n(t^{III}) = s_n'\right) = \xi^{\tau}\left(s_n, s_n', X_n^{\tau}, \hat{\theta}^{\tau}, \hat{\varepsilon}^{\tau}, \hat{\phi}_n^{\tau}\right). \quad (6)$$

where $\xi^{\tau}(\cdot)$ denotes the probabilistic deterioration progress between $\hat{S}_n(t^{III})$ and $\hat{S}_n((t+1)^I)$; X_n^{τ} the set of facility-specific influential factors (e.g., traffic loading, structural number); $\hat{\Theta}^{\tau}$ the set of systemwide parameters; $\hat{\varepsilon}^{\tau}$ the set of systemwide model uncertainties; and $\hat{\phi}_n^{\tau}$ the set of facility-specific uncertainties. The model parameters $\hat{\Theta}^{\tau}$ and uncertainties, $\hat{\varepsilon}^{\tau}$ and $\hat{\phi}_n^{\tau}$, are updated sequentially at every decision-making time step, τ, based upon the inspection data collected until τ from all N facilities.

To calculate the probability of the initial condition in the current period, $\hat{p}^{\tau}(S_n(0^I) = s_n)$ (which will be used in **Formula (3)**), we need to trace back to the last inspection or M&R activity before τ. Suppose that inspection or M&R activity occurred in a period τ_n^0 earlier than the current period. Then the belief of the initial condition in period τ, $S_n(0^I)$, is calculated based on the latest condition $S_n^{\tau_n^0}(0^{III})$:

$$\hat{p}^{\tau}\left(S_n(0^I) = s_n | S_n^{\tau_n^0}(0^{III}) = s_n'\right) = \sum_{s_n^{\tau-1}\in\mathbb{S}_n}\sum_{s_n^{\tau-2}\in\mathbb{S}_n}\cdots\sum_{s_n^{\tau_n^0+1}\in\mathbb{S}_n}\xi^{\tau}\left(s_n, s_n^{\tau-1}, X_n^{\tau-1}, \hat{\Theta}^{\tau}, \hat{\varepsilon}^{\tau}, \hat{\phi}_n^{\tau}\right)\times \xi^{\tau}\left(s_n^{\tau-1}, s_n^{\tau-2}, X_n^{\tau-2}, \hat{\Theta}^{\tau}, \hat{\varepsilon}^{\tau}, \hat{\phi}_n^{\tau}\right)\times\cdots\times\xi^{\tau}\left(s_n^{\tau_n^0+1}, s_n', X_n^{\tau_n^0}, \hat{\Theta}^{\tau}, \hat{\varepsilon}^{\tau}, \hat{\phi}_n^{\tau}\right), \quad (7)$$

where s_n' is the deterministic condition either observed by inspection or achieved by an M&R activity at τ_n^0 before the current time point τ.

3.2 Optimization formulation

The objective of the optimization problem at the current decision-making time τ is to minimize the discounted sum of the expected user costs $J_{[0,T]}$ under the combined agency budget constraint for all the pavement facilities $n = 1,2,\dots,N$ over the planning horizon $[0,T]$. We present the objective function in Section 3.2.1 and the budget constraint in Section 3.2.2.

3.2.1 Objective function

The objective function, $J_{[0,T]}\left(S(0^I)\right)$ ($\equiv \sum_n J_{n,[0,T]}\left(S_n(0^I)\right)$), comprises the discounted user costs during all $t = 0,\dots,T-1$ as shown in **Equation (8)**. The user cost during period t consists of two

components: (i) the cost due to pavement serviceability, $u = \sum_{n=1,\dots,N} u_n$, where u_n is a function of the pavement condition $S_n(t^{III})$; and (ii) the cost due to the work-zone impact of M&R activities, $w = \sum_{n=1,\dots,N} w_n$, where w_n is a function of the M&R activity $\boldsymbol{y}_n(t^{II})$ and the pavement condition before M&R, $S_n(t^{II})$. We define $S(t^{III}) = \{S_n(t^{III}), \forall n\}$, $S(t^{II}) = \{S_n(t^{II}), \forall n\}$, and $\boldsymbol{y}(t^{II}) = \{\boldsymbol{y}_n(t^{II}), \forall n\}$. Then we have:

$$J_{[0,T]}\big(S(0^I)\big) = \sum_{t=0}^{T-1} \alpha^t \cdot \big\{u\big(S(t^{III})\big) + w\big(S(t^{II}), \boldsymbol{y}(t^{II})\big)\big\}, \tag{8}$$

where the initial condition $S(0^I) = \{S_n(0^I), \forall n\}$; and $\alpha \in (0,1]$ stands for the discounting factor. Note that $S(t^{III})$ is a function of $S(t^{II})$ and $\boldsymbol{y}(t^{II})$; see Section 3.1.3.

However, we do not know the true conditions $S(t^I)$, and even $S(t^{II})$ and $S(t^{III})$ when no inspection is performed in a period. Thus, our best effort is to use the belief $\hat{d}^\tau$ estimated using historical inspection data and the belief $\hat{p}^\tau\big(S_n(t^I)\big)$ derived based on the belief $\hat{d}^\tau$. We then minimize the *predicted* total discounted costs instead, which is represented by $J_{[0,T]}\left(\hat{S}(0^I)\right)$ or $\hat{J}_{[0,T]}$ as shown in **Equation (9)**. The condition-based forms of $\boldsymbol{x}_n$ and $\boldsymbol{y}_n$ (see **Formulae (3)** and **(5)**) are used in the objective function.

$$\hat{J}^*_{[0,T]} = \min_{\boldsymbol{x},\boldsymbol{y}} \mathop{\mathrm{E}}_{\substack{\hat{S}_n(t^I),\\ \forall n,t}} \left[\sum_{t=0}^{T-1} \alpha^t \cdot \sum_{n=1}^{N} \left\{u_n\left(\hat{S}_n(t^{III})\right) + w_n\left(\hat{S}_n(t^{II}), \boldsymbol{y}_n\left(t^{II}\middle|\hat{S}_n(t^I), \boldsymbol{x}_n\left(t^I\middle|\hat{p}^\tau(S_n(t^I))\right)\right)\right)\right\}\right], \tag{9}$$

where $\hat{S}_n(t^{II})$ and $\hat{S}_n(t^{III})$ represent the best estimates of pavement conditions at t^{II} and t^{III}, respectively[1]; $\boldsymbol{x}(t^I) = \{\boldsymbol{x}_n(t^I), \forall n\}$; and operator E[·] takes the expected value.

3.2.2 Agency budget constraint

It is reasonable to assume that flexible budget allocation and transfer are allowed within a planning horizon under a given average annual budget. Thus, the budget constraint is presented in **Constraint (10)**.

[1] With a slight abuse of notations, we specify that $\hat{S}_n(t^{II})$ and $\hat{S}_n(t^{III})$ in **Equation (9)** are equal to the true conditions $S_n(t^{II})$ and $S_n(t^{III})$, respectively, if an inspection is performed in period t.

$$\hat{A}_{[0,T]} = \underset{\hat{S}_n(t^I),\forall n,t}{\mathrm{E}}\left[\sum_{t=0}^{T-1}\alpha^t \cdot \sum_{n=1}^{N}\left\{ci_n \cdot \boldsymbol{x}_n\left(t^I\middle|\hat{p}^\tau\left(S_n(t^I)\right)\right) + cm_n\left(\boldsymbol{y}_n\left(t^{II}\middle|\hat{S}_n(t^I), \boldsymbol{x}_n\left(t^I\middle|\hat{p}^\tau\left(S_n(t^I)\right)\right)\right)\right)\right\}\right] \leq \frac{1-\alpha^T}{1-\alpha}B^\tau, \quad (10)$$

where $\hat{A}_{[0,T]}(=\sum_{n=1,\dots,N}\hat{A}_{n,[0,T]})$ is the expected total discounted agency cost for the entire pavement system over a given planning horizon $[0,T]$ at the current time τ; B^τ is the annual average budget for the planning horizon known at τ; ci_n is the unit inspection cost for facility n, which must vary with the facility's characteristics, e.g., the lane length; and $cm_n(\cdot)$ is the M&R cost for facility n under the DCB M&R option $\boldsymbol{y}_n$. Under certain operating conditions, the inspection method and cost would depend on the predicted pavement condition $\hat{S}_n(t^I)$. For example, a severely damaged facility may need to be inspected via more intensive methods. In this case, the unit inspection cost ci_n is not a constant value but a function of $\hat{S}_n(t^I)$, i.e., $ci_n\left(\hat{S}_n(t^I)\right)$. It is also stochastic since the input $\hat{S}_n(t^I)$ is stochastic. Nevertheless, we choose to use a constant ci_n as in Shon and Lee (2021) for simplicity.[2]

4. SOLUTION METHODOLOGY

This section proposes a bottom-up solution methodology for the stochastic system-level optimization problem, which can handle facility-specific features and the influence of future budget on the current inspection and M&R decisions. We first decompose the system-level problem into multiple facility-level problems by introducing a Lagrange multiplier in Section 4.1. The solution method for each facility-level problem is presented in Section 4.2. Finally, Section 4.3 solves the Lagrange problem presented in Section 4.1.

4.1 System-level problem decomposition

We decompose the weakly coupled system-level problem, defined by the objective function in **Equation (9)** and **Constraint (10)**, into N facility-level subproblems by relaxing the budget

[2] With modest modifications, our optimization framework can incorporate stochastic and condition-based inspection cost models if they are available or can be calibrated by available data. (Unfortunately, those models and data are rare in the literature.) We believe our main findings would still hold if more complicated inspection cost functions were used, since the inspection cost only takes up a small portion of the system cost, as we shall see momentarily.

constraint. To this end, we introduce the non-negative Lagrange multiplier, $\boldsymbol{\lambda}$, and the corresponding Lagrange function is shown below:

$$L(\boldsymbol{x}, \boldsymbol{y}|\boldsymbol{\lambda}) = \hat{J}_{[0,T]}(\boldsymbol{x}, \boldsymbol{y}) + \boldsymbol{\lambda} \cdot \left(\hat{A}_{[0,T]}(\boldsymbol{x}, \boldsymbol{y}) - \frac{1-\alpha^T}{1-\alpha} B^\tau\right). \tag{11}$$

The original system-level optimization problem can be converted into its Lagrange dual problem, defined as:

$$L^* = \sup_{\boldsymbol{\lambda}} L^*|\boldsymbol{\lambda} = \sup_{\boldsymbol{\lambda}} \min_{\boldsymbol{x},\boldsymbol{y}|\lambda} L(\boldsymbol{x}, \boldsymbol{y}|\boldsymbol{\lambda}). \tag{12}$$

In **Equation (12)**, the decision variables are $\{\boldsymbol{\lambda}; \boldsymbol{x}, \boldsymbol{y}\}$. A bi-level approach can be used to find the optimal solution. In the lower-level problem, we optimize the Lagrange function for the management policy $\boldsymbol{x}$ and $\boldsymbol{y}$ as shown in **Equation (13)** when $\boldsymbol{\lambda}$ is given. In the upper-level problem, we find the optimal Lagrange multipliers $\boldsymbol{\lambda}^*$ for maximizing $L^*|\boldsymbol{\lambda}$. The lower-level problem is separable since the interdependence among facilities is removed by relaxing the budget constraint. For any given λ, the optimal dual policy $\{\boldsymbol{x}^*, \boldsymbol{y}^*|\boldsymbol{\lambda}\}$ is the combination of the facility-level optimal dual policies $\{\boldsymbol{x}_n^*, \boldsymbol{y}_n^*|\boldsymbol{\lambda}\}$ for all n:

$$\{\boldsymbol{x}^*, \boldsymbol{y}^*|\boldsymbol{\lambda}\} = \left\{\underset{\boldsymbol{x},\boldsymbol{y}}{\operatorname{argmin}} L(\boldsymbol{x}, \boldsymbol{y}|\boldsymbol{\lambda})\right\} = \left\{\underset{\boldsymbol{x}_n,\boldsymbol{y}_n}{\operatorname{argmin}} H_n(\boldsymbol{x}_n, \boldsymbol{y}_n|\lambda), \forall n\right\}, \tag{13}$$

where $H_{n,[0,T]}(\boldsymbol{x}_n, \boldsymbol{y}_n|\boldsymbol{\lambda}) \equiv \hat{J}_{n,[0,T]}(\boldsymbol{x}_n, \boldsymbol{y}_n) + \boldsymbol{\lambda} \cdot \hat{A}_{n,[0,T]}(\boldsymbol{x}_n, \boldsymbol{y}_n), \forall n.$

4.2 Facility-level solution method

Given λ, the objective of **Equation (13)** at the current time τ is to find the optimal policies at $t = 0$; i.e., for each facility n, find $\boldsymbol{x}_n^*\left(0^I|\hat{p}^\tau\left(\hat{S}_n(0^I) = s_n\right), \forall s_n \in \mathbb{S}_n\right)$ and $\boldsymbol{y}_n^*\left(0^{II}|\tilde{S}_n(0^{II}) = s_n, \boldsymbol{x}_n(0^I) = 1\right)$ for all s_n. We propose a 3-step dynamic programming algorithm detailed as follows to solve this facility-level problem:

Step 1. Solve the Bellman equation by backward induction from $t = T - 1$ to $t = 0$. At each step, find the optimal DCB M&R action and the optimal time of the next SCB inspection for all possible states $s_n \in \mathbb{S}_n$. This step is detailed as follows.

The Bellman equation at time t is presented in **Equation (14)**. At this step, we aim to find the optimal expected cost-to-go starting from t^{II}, given that an inspection was conducted at t^I (i.e., $\boldsymbol{x}_n(t^I) = 1$) and the current pavement condition is revealed as s_n. The decisions include the optimal M&R action at t^{II}, $\boldsymbol{y}_n\left(t^{II} | \hat{S}_n(t^{II}) = s_n, \boldsymbol{x}_n(t^I) = 1\right)$ (simplified as $\boldsymbol{y}_n(t^{II})$ in what follows) and the optimal time of the next inspection, $t + \boldsymbol{\Delta}_n(t)$, where $\boldsymbol{\Delta}_n(t)$ is a positive integer and indicates the time gap between time t and the time of the next inspection if $\boldsymbol{x}_n(t^I) = 1$. The inspection decision is based on the stochastic belief of $\hat{S}_n\left(\left(t + \boldsymbol{\Delta}_n(t)\right)^I\right)$.

The RHS of the Bellman equation consists of the following components:

- The user costs occurring in period t: $u_n\left(f\left(s_n, \boldsymbol{y}(t^{II})\right)\right) + w_n\left(s_n, \boldsymbol{y}(t^{II})\right)$;
- The expected discounted user costs from period $t+1$ to $t + \boldsymbol{\Delta}_n(t)$: $\sum_{\mu=1}^{\boldsymbol{\Delta}_n(t)-1} \alpha^{\mu} \cdot u_n\left(\hat{S}((t+\mu)^I)\right)$, which is zero if an inspection is carried out at $t+1$, i.e., $\boldsymbol{\Delta}_n(t) = 1$;
- The agency costs, including the M&R cost applied at t and the discounted inspection cost applied at $t + \boldsymbol{\Delta}_n(t)$, multiplied by λ: $\lambda \cdot \left\{cm_n\left(\boldsymbol{y}_n(t^{II})\right) + \alpha^{\boldsymbol{\Delta}_n(t)} \cdot ci_n\right\}$;
- The expected discounted cost-to-go at $t + \boldsymbol{\Delta}_n(t)$: $\alpha^{\boldsymbol{\Delta}_n(t)} \cdot \underset{\hat{S}_n\left(\left(t+\boldsymbol{\Delta}_n(t)\right)^{II}\right)}{\mathrm{E}} \left[H^*_{[t+\boldsymbol{\Delta}_n(t),T]}\left(\hat{S}_n\left(\left(t+\boldsymbol{\Delta}_n(t)\right)^{II}\right) | \boldsymbol{x}_n\left(\left(t+\boldsymbol{\Delta}_n(t)\right)^I\right) = 1\right)\right]$.

As an exception, at the last step $t = T - 1$, no future inspection will be considered. This special case is modeled using **Equation (15)**.

$$H^*_{[t,T]}\left(\hat{S}_n(t^{II}) = s_n | \boldsymbol{x}_n(t^I) = 1\right) = \min_{\boldsymbol{y}_n(t^{II}), \boldsymbol{\Delta}_n(t)} \Bigg\{ u_n\left(f\left(s_n, \boldsymbol{y}_n(t^{II})\right)\right) + w_n\left(s_n, \boldsymbol{y}_n(t^{II})\right) + \sum_{\mu=1}^{\boldsymbol{\Delta}_n(t)-1} \underset{\hat{S}_n((t+\mu)^I)}{\mathrm{E}} \left[\alpha^{\mu} \cdot u_n\left(\hat{S}_n((t+\mu)^I)\right)\right] + \boldsymbol{\lambda} \cdot \left\{cm_n\left(\boldsymbol{y}_n(t^{II})\right) + \right. \tag{14}$$

$$\alpha^{\boldsymbol{\Delta}_n(t)} \cdot ci_n\} + \alpha^{\boldsymbol{\Delta}_n(t)} \cdot \underset{\hat{S}_n\left((t+\boldsymbol{\Delta}_n(t))^{II}\right)}{\mathrm{E}}\left[H^*_{[t+\boldsymbol{\Delta}_n(t),T]}\left(\hat{S}_n\left((t+\boldsymbol{\Delta}_n(t))^{II}\right)|\boldsymbol{x}_n\left((t+\boldsymbol{\Delta}_n(t))^{I}\right)=1\right)\right]\Bigg\}, \forall s_n \in \mathbb{S}_n, t = T-2,\dots,0;$$

$$H^*_{[t,T]}\left(\hat{S}_n(t^{II}) = s_n|\boldsymbol{x}_n(t^I)=1\right) = \min_{\boldsymbol{y}_n(t^{II})}\Big\{u_n\left(f\left(s_n,\boldsymbol{y}_n(t^{II})\right)\right) + w_n\left(s_n,\boldsymbol{y}_n(t^{II})\right) + \boldsymbol{\lambda}\cdot \left\{cm_n\left(\boldsymbol{y}_n(t^{II})\right)\right\} + \alpha\cdot \underset{\hat{S}_n(T)}{\mathrm{E}}\left[TC\left(\hat{S}_n(T)\right)\right]\Big\}, \forall s_n \in \mathbb{S}_n, t = T-1. \quad (15)$$

where $TC\left(\hat{S}_n(T)\right)$ refers to the terminal cost under condition $\hat{S}_n(T)$.

The following constraint applies to $\boldsymbol{\Delta}_n(t)$:

$$t + \boldsymbol{\Delta}_n(t) \le T-1, \forall t = T-2,\dots,0. \quad (16)$$

Step 2. Consider the case where no inspection is performed at $t = 0^I$ (i.e., $\boldsymbol{x}_n(0^I) = 0$). This leads to a different Bellman equation for calculating the expected future cost under a specific condition of $\hat{S}_n(0^{II}) = s_n, \forall s_n \in \mathbb{S}_n$; see **Equation (17)**. Without the inspection at $t = 0^I$, the following M&R action must be "do-nothing," and the only decision variable is the time of the next inspection, $\boldsymbol{\Delta}_n(0)$. The work-zone-related cost and M&R cost at $t = 0$, are also removed from the RHS of **Equation (17)**.

$$H^*_{[0,T]}\left(\hat{S}_n(0^{II}) = s_n|\boldsymbol{x}_n(0^I)=0\right) = \min_{\boldsymbol{\Delta}_n(0)}\Big\{u_n\left(f\left(s_n,\boldsymbol{y}_n(0^{II})\right)\right) + \sum_{\mu=1}^{\boldsymbol{\Delta}_n(0)-1}\underset{\hat{S}_n((\mu)^I)}{\mathrm{E}}\left[\alpha^{\mu}\cdot u_n\left(\hat{S}_n(\mu^I)\right)\right] + \lambda\cdot\alpha^{\boldsymbol{\Delta}_n(0)}\cdot ci_n + \alpha^{\boldsymbol{\Delta}_n(0)}\cdot \underset{\hat{S}_n(\boldsymbol{\Delta}_n(0)^{II})}{\mathrm{E}}\left[H^*_{[\boldsymbol{\Delta}_n(0),T]}\left(\hat{S}_n(\boldsymbol{\Delta}_n(0)^{II})|\boldsymbol{x}_n(\boldsymbol{\Delta}_n(0)^I)=1\right)\right]\Big\}, \forall s_n \in \mathbb{S}_n. \quad (17)$$

Step 3. Now the only remaining decision variable is $\boldsymbol{x}_n(0^I)$, i.e., whether to perform an inspection at $t = 0^I$ or not. The model is shown in **Equation (18)**.

$$\boldsymbol{x}_n^*(0^I) = \underset{\boldsymbol{x}_n(0^I)\in\{0,1\}}{\operatorname{argmin}} \Big\{ \underset{\hat{S}_n(0^I)}{\mathrm{E}}\big[H^*_{[0,T]}\big(\hat{S}_n(0^{II}) = s_n|\boldsymbol{x}_n(0^I) = 1\big)\big] + ci_n, \underset{\hat{S}_n(0^I)}{\mathrm{E}}\big[H^*_{[0,T]}\big(\hat{S}_n(0^{II}) = s_n|\boldsymbol{x}_n(0^I) = 0\big)\big] \Big\}. \tag{18}$$

The first term in the braces is the expected value of **Equation (14)** at $t = 0$ plus the inspection cost at $t = 0$; see **Equation (19)**. The second term is the expected value of **Equation (17)**.

$$\underset{\hat{S}_n(0^I)}{\mathrm{E}}\big[H^*_{[0,T]}\big(\hat{S}_n(0^{II}) = s_n|\boldsymbol{x}_n(0^I) = 1\big)\big] + ci_n = \textstyle\sum_{s_n\in\mathbb{S}_n} \hat{p}^{\tau}\big(\hat{S}_n(0^I) = s_n\big) \cdot H^*_{[0,T]}\big(\hat{S}_n(0^{II}) = s_n|\boldsymbol{x}_n(0^I) = 1\big) + ci_i. \tag{19}$$

$$\underset{\hat{S}_n(0^I)}{\mathrm{E}}\big[H^*_{[0,T]}\big(\hat{S}_n(0^{II}) = s_n|\boldsymbol{x}_n(0^I) = 0\big)\big] = \textstyle\sum_{s_n\in\mathbb{S}_n} \hat{p}^{\tau}\big(\hat{S}_n(0^I) = s_n\big) \cdot H^*_{[0,T]}\big(\hat{S}_n(0^{II}) = s_n|\boldsymbol{x}_n(0^I) = 0\big). \tag{20}$$

Note that $\hat{p}^{\tau}\big(\hat{S}_n(0^I) = s_n\big)$ is estimated using **Equation (7)**.

Equation (18) determines the optimal inspection strategies for all N facilities with a given λ. The above dynamic programming algorithm guarantees a globally optimal solution. However, its computational cost is polynomial to the size of the system, i.e., $\mathcal{O}(N \cdot T \cdot |\mathbb{S}_n|)$. For better computational tractability, we can solve the problem in Step 1 (**Equations (14-16)**) using Approximate Dynamic Programming (ADP). The details of the ADP solution algorithm are presented in **Appendix B.**

4.3 Numerical algorithm for the Lagrange problem

With the solutions to every facility-level problem, the Lagrange dual problem (**Equation (12)**) is reduced to searching for the optimal Lagrange multiplier, i.e.,

$$\begin{aligned} L^* &= \sup_{\boldsymbol{\lambda}} L^*|\boldsymbol{\lambda} \\ &= \sup_{\boldsymbol{\lambda}} \Big[\textstyle\sum_{n=1}^{N} \underset{\hat{S}_n(0^I)}{\mathrm{E}}\big[H^*_n\big(\hat{S}_n(0^{II})|\boldsymbol{\lambda}\big)\big] - \boldsymbol{\lambda}\frac{1-\alpha^T}{1-\alpha}B\Big]. \end{aligned} \tag{21}$$

Computing the derivatives of $L^*|\boldsymbol{\lambda}$ with respect to $\boldsymbol{\lambda}$ is often computationally inefficient due to the complicated mathematical forms of M&R effectiveness and cost models. Hence, we update the Lagrange multiplier using a gradient approximation algorithm. The algorithm is relegated to **Appendix C**.

The above solution procedure produces the optimal inspection and M&R actions for all facilities in the current period τ. If an inspection is performed, the deterioration model will be updated using the new inspection data before repeating the optimization for the next period $\tau + 1$. Many statistical learning methods can be used to update the deterioration model $\hat{p}^{\tau}$. A maximum likelihood method will be used to update the specific deterioration model used in Section 5. The method is relegated to **Appendix D** (Zhang, 2019).

5. NUMERICAL STUDY

We consider a pavement system consisting of 50 heterogeneous facilities. Each facility exhibits several characteristics, including structural number, traffic loading, and initial condition states. All the numerical cases presented in this section are carried out by Matlab R2016a on a PC with Inter® Xeon® 3.60 GHz CPU, 32.0GB RAM, and Windows 10 Pro 64-bit. The facility-level problem is solved by ADP. The specific deterioration model is presented in Section 5.1. The cost and M&R performance models are furnished in Section 5.2. Parameter values used in the case studies are introduced in Section 5.3. Section 5.4 presents and discusses the numerical results and findings.

5.1 Deterioration model

The facility-level condition state $S_n(t)$ is defined as a bi-dimensional vector consisting of the pavement surface roughness $R_n(t)$ and pavement age $Age_n(t)$, i.e., $S_n(t) = \{R_n(t), Age_n(t)\}$. Here $Age_n(t) \in \{0,1, \dots, h^{max}\}$ is counted from the year of pavement construction or its last reconstruction, where h^{max} is the maximum allowable age. **Equation (22)** describes the roughness and age progression model from t^{III} to $(t+1)^I$ (recall that the durations of t^I and t^{II} are negligible), which has been commonly used in the literature (Paterson, 1990).

$$\hat{r}_n((t+1)^I) = r_n(t^{III})e^{\hat{\Theta}_\tau^1} + \hat{\Theta}_\tau^2 l_n(1+SN_n)^{\hat{\Theta}_\tau^3} e^{\hat{\Theta}_\tau^1 (Age_n(t^{III})+1)} + \hat{\varepsilon}^{\tau}; \tag{22a}$$

$$Age_n((t+1)^I) = Age_n(t^{III}) + 1. \quad (22b)$$

where $r_n(t) \in [r^{new}, r^{max}]$ is a continuous roughness value at t. The facility-specific influential factor X_n^τ in **Equation (6)** consists of the traffic loading l_n and structural number SN_n in **(22a)**[3]; the systemwide parameter set $\hat{\Theta}^\tau$ in **(6)** includes $\hat{\Theta}_\tau^1$, $\hat{\Theta}_\tau^2$ and $\hat{\Theta}_\tau^3$ in **(22a)**; $\hat{\varepsilon}^\tau$ represents the systemwide random error term in deterioration from t to $t+1$, with zero mean and variance of $\hat{\sigma}_\tau^2$; the facility-specific uncertainty term $\hat{\phi}_n^\tau$ in **(6)** does not apply here. We assume that the error terms for different periods are independent and identically distributed random variables.

To discretize the roughness index, we divide its range $[r^{new}, r^{max}]$ into M equal-sized bins indexed by $m = 1, 2, \ldots, M$. The size of each bin is denoted by $\delta = \frac{r^{max} - r^{new}}{M}$. The midpoint of the m-th bin, denoted by $r^m = r^{new} + (m - 0.5)\delta$, is used to represent the roughness index that falls in this bin. Thus, the size of the state set $|\mathbb{S}_n| = M \cdot (1 + h^{max})$.

The discrete deterioration probability, $\hat{p}\left(\hat{S}_n((t+1)^I) = s_n | S_n(t^{III}) = s_n'\right)$, where $s_n = \{r^m, h\}, s_n' = \{r^{m'}, h'\}$, is calculated as:

$$\hat{p}^\tau\left(\hat{R}_n((t+1)^I) = r^m, Age_n((t+1)^I) = h | R_n(t^{III}) = r^{m'}, Age_n(t^{III}) = h'\right) = Prob\left(r^{m'} e^{\Theta_\tau^1} + \Theta_\tau^2 l_n (1 + SN_n)^{\Theta_\tau^3} e^{\Theta_\tau^1 (h'+1)} + \varepsilon_\tau \in [r^m - 0.5\delta, r^m + 0.5\delta)\right), \text{if } h = h' + 1 \quad (23a)$$

$$\hat{p}^\tau = 0, \text{otherwise.} \quad (23b)$$

Equation (23b) specifies that the pavement age must increase by one from t^{III} to $(t+1)^I$. If a reconstruction activity is conducted at t^{II}, the age will be reset to zero. This would be captured in the reconstruction performance model; see the next section.

Based on a known distribution of $\hat{\varepsilon}^\tau$, $\hat{p}^\tau$ is found for $M^2 \cdot (1 + h^{max})^2$ pairs of $S_n(t^{III})$ and $\hat{S}_n((t+1)^I)$. The model parameters, $\hat{\Theta}_\tau^1$, $\hat{\Theta}_\tau^2$, $\hat{\Theta}_\tau^3$, and $\hat{\sigma}_\tau^2$, are updated sequentially at every decision-making time step, τ, based upon the inspection data that have been collected before τ. A maximum-likelihood method used for updating these parameters is furnished in **Appendix D**.

5.2 Cost and performance models

[3] In our numerical cases, l_n and SN_n are assumed to be known constants for each facility n; i.e., they will not be updated.

Two types of M&R activities are considered: rehabilitation and reconstruction. The associated decision variables are $\boldsymbol{y}_n(t^{II}) = \{\boldsymbol{\varpi}_{n,t}, \boldsymbol{\chi}^1_{n,t}, \boldsymbol{\chi}^2_{n,t}\}$, where the binary variables $\boldsymbol{\chi}^1_{n,t}$ and $\boldsymbol{\chi}^2_{n,t}$ are equal to 1 if a rehabilitation or reconstruction activity is executed in period t for facility n, respectively, and 0 otherwise; and $\boldsymbol{\varpi}_{n,t}$ denotes the rehabilitation intensity. The 'do-nothing' option is represented by $\{\boldsymbol{\varpi}_{n,t} = 0, \boldsymbol{\chi}^1_{n,t} = 0, \boldsymbol{\chi}^2_{n,t} = 0\}$. The full facility-level cost and performance models are borrowed from previous studies (e.g., Ouyang and Madanat, 2006) and presented below:

$$u_n\big(S_n(t^{III})\big) = l_n\big(c_{n,1}R_n(t) + c_{n,2}\big); \tag{24a}$$

$$w_n(\cdot) = \boldsymbol{\chi}^2_{n,t} \cdot \beta_n l_n; \tag{24b}$$

$$cm_n\big(\boldsymbol{y}_n(t^{II})\big) = \boldsymbol{\chi}^1_{n,t}\big(\gamma_{n,1}\boldsymbol{\varpi}_{n,t} + \gamma_{n,2}\big) + \boldsymbol{\chi}^2_{n,t}\big(z_{n,1} + z_{n,2}l_n\big); \tag{24c}$$

$$R_n(t^{III}) = f\big(R_n(t^{II}), \boldsymbol{\varpi}_{n,t}, \boldsymbol{\chi}^1_{n,t}, \boldsymbol{\chi}^2_{n,t}\big) \tag{24d}$$

$$= R_n(t^{II}) - \boldsymbol{\chi}^1_{n,t} \cdot G\big(R_n(t^{II}), \boldsymbol{\varpi}_{n,t}\big) + \boldsymbol{\chi}^2_{n,t} \cdot \big(r^{new} - R_n(t^{II})\big);$$

$$G\big(R_n(t^{II}), \boldsymbol{\varpi}_{n,t}\big) = \frac{g^1 R_n(t^{II})}{g^2 R_n(t^{II}) + g^3}\boldsymbol{\varpi}_{n,t}; \tag{24e}$$

$$0 \le \boldsymbol{\varpi}_{n,t} \le g^2 R_n(t^{II}) + g^3; \tag{24f}$$

$$\boldsymbol{\chi}^1_{n,t} + \boldsymbol{\chi}^2_{n,t} \le 1; \tag{24g}$$

$$Age_n(t^{III}) = Age_n(t^{II})\big(1 - \boldsymbol{\chi}^2_{n,t}\big); \tag{24h}$$

$$r^1 \le R_n(t) \le r^M; \tag{24i}$$

$$0 \le Age_n(t) \le h^{max}; \tag{24j}$$

The models for user cost and agency costs for M&R activities in period t for facility n are described in **Equations (24a-c)**, where $c_{n,1}, c_{n,2}, \beta_n, \gamma_{n,1}, \gamma_{n,2}, z_{n,1}$ and $z_{n,2}$ are non-negative cost coefficients. We assume the work-zone cost for rehabilitation is zero. **Constraint (24d)** provides the function f (see Section 3.1.3) that governs the roughness reduction from a rehabilitation or reconstruction activity.[4] Function G represents the rehabilitation effectiveness as defined in **Equation (24e)**, where g^1, g^2, and g^3 are model coefficients. **Constraint (24f)** stipulates the upper bound for the rehabilitation intensity $\boldsymbol{\varpi}_{n,t}$. **Constraint (24g)** ensures that at most one activity is applied in one period. **Constraint (24h)** ensures that the pavement age is reset to 0 after

[4] With a slight abuse of notation, the same notation f is used in **(24d)** to denote the change of roughness index, while in Section 3.1.3, f represents the change of pavement state.

a reconstruction. **Constraints (24i-j)** specify the upper and lower bounds of the roughness level and the pavement age.

5.3 PARAMETER VALUES

Table 1 summarizes the parameter values used in our numerical cases, which are extracted from empirical studies and real-world experiments (Shon and Lee, 2021; Zhang et al., 2017; Ouyang and Madanat, 2006; Gu et al., 2012; Lee and Madanat, 2015; Lee et al., 2016). To account for the heterogeneity among facilities, we generate the traffic loading, structural number, and cost coefficients of each facility using predefined distributions as presented in **Table 1**, where $U[a, b]$ denotes a uniform distribution from a to b, and $\Gamma[a, b]$ a uniform distribution of *integer* random variables from a to b. Additionally, the time of the last M&R activity conducted on facility n before the present time ($\tau = 0$), τ_n^0, is randomly generated from $\Gamma[-1, -3]$. The roughness index and pavement age at time τ_n^0 are also generated from uniform distributions: $R_n^{\tau_n^0}(0) \sim U[1, 3]$, and $Age_n^{\tau_n^0}(0) \sim \Gamma[0, 30],\ \forall n = 1,2, \cdots, N$.[5]

TABLE 1. Parameter values.

Parameter	Value	Unit	Description
$c_{n,1}$	$U[6.5E3, 7.2E3]$	\$/IRI/km/lane/million ESAL	User cost rates due to serviceability
$c_{n,2}$	0	-	
$\gamma_{k,1}$	$U[1.4E3, 1.9E3]$	\$/mm/km/lane	Rehabilitation cost rates
$\gamma_{k,2}$	$U[1.7E4, 2.5E4]$	\$/km/lane	
ci_n	$U[1.1E3, 1.3E3]$	\$/km/lane	Inspection cost rate
SN_n	$\Gamma[7, 11]$	SN	Structural number
g^1	0.66	-	Rehabilitation effectiveness model coefficients
g^2	7.15	mm/IRI	
g^3	18.3	mm	
α	0.9524	-	Discount rate
$z_{n,1}$	180,000	\$/km/lane	Reconstruction cost rates
$z_{n,2}$	227,000	\$·year/km/million ESAL	
l_n	$U[0.4, 0.9]$	million ESAL/year/lane	Traffic loading
r^{new}	0.75	IRI	Bounds of pavement roughness level
r^{max}	6	IRI	
h^{max}	60	year	Maximum lifecycle length

[5] Uniform distributions have been commonly used to generate facility-specific parameters of a pavement system (ref.) when real operation data are unavailable.

T	20	year	Planning horizon
N	50	-	Number of facilities
M	21	-	Number of discretized bins for roughness level
θ^1	0.04	-	
θ^2	930	-	Deterioration model coefficients
θ^3	-5	-	
σ^2	0.25	-	Variance of the deterioration model's error term

5.4 OPTIMIZATION RESULTS

We first examine the solution of the condition-based joint optimization of inspection and M&R policies for $T = 20$ years. Section 5.4.1 presents the optimal user and agency cost components against the budget obtained for a one-off optimization at $\tau = 0$. Section 5.4.2 applies our method to 20 consecutive years (i.e., $\tau = 0, 1, \dots, 19$) and plots the trajectories of inspection and M&R actions for selected individual facilities. Since the belief updating process and the condition-based inspection scheduling are two methodological novelties of this paper, their effects on the system cost are examined in Sections 5.4.3 and 5.4.4, respectively. A sensitivity analysis of the unit inspection cost is furnished in Section 5.4.5. Finally, Section 5.4.6 examines the computation efficiency of our solution method for a one-off optimization at $\tau = 0$.

5.4.1 Effects of budget on user and agency costs

At $\tau = 0$, the optimal expected user cost (the objective) and agency cost components are plotted against the combined annual budget $B^0 \in [4.5 \times 10^5, 7.5 \times 10^5]$ \$/year in **Figure 3**. Note here that the optimal cost includes the discounted future cost for $T = 20$ years, given the present uncertainty belief.

As expected, the optimal user cost (the dashed curve with triangle markers) decreases as the budget grows. The reconstruction cost (the dot-marked solid curve) clearly increases with the budget, indicating that more frequent reconstructions will be applied to improve the serviceability if the budget permits. However, the rehabilitation cost (the square-marked solid curve) exhibits a different trend. Though it increases with B^0 when the budget is sufficiently large, a decreasing trend is observed when the budget is small (which is more likely the case in the near future). It turns out that more frequent rehabilitations will be performed to postpone the costly recontructions when the budget is highly limited (Zhang et al., 2017). Also note that the reconstruction cost under the minimum budget in **Figure 3** is quite low, and it grows rapidly as the rehabilitation cost

559 diminishes for $B^0 < 5.25 \times 10^5$ \$. Regarding the inspection cost (the diamond-marked solid
560 curve), it is found to be fairly insensitive to the budget. Relatively larger inspection costs are
561 observed at the two ends of the budget range. This is because more inspections are needed to guide
562 more frequent M&R activities (more rehabilitations when the budget is low) in those cases.
563

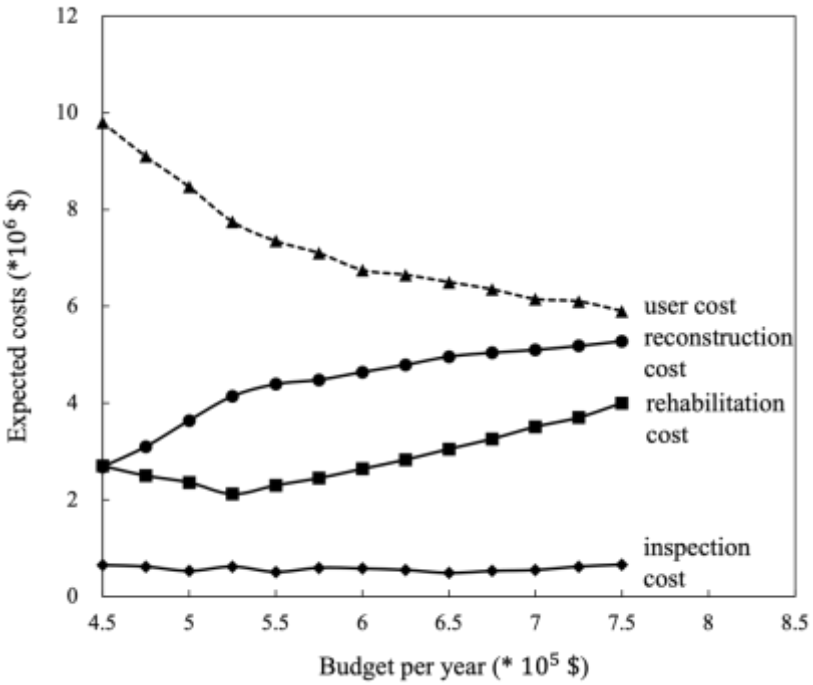

564

565 **Figure 3. Effects of the combined agency budget on system-level optimal costs.**

566

567 *5.4.2 Effects of budget and initial condition on the optimal policies of individual facilities*

568 To examine how the budget affects the optimal inspection and M&R plans for individual facilities,
569 we compare realizations of the optimal policies under two annual budget values: (i) $B^\tau \equiv B =$
570 7×10^5 \$/year (adequate budget) (**Figure 4a**) and (ii) $B^\tau \equiv B = 5 \times 10^5$ \$/year (inadequate
571 budget) (**Figure 4b**), $\forall \tau$. Under each budget, we repeat the optimization for 20 consecutive years,
572 i.e., $\tau \in \{0, 1, \dots, 19\}$. Three facilities are selected for analysis: a good and new facility with initial
573 condition $\left(R_n^0(0^I), Age_n^0(0^I)\right) = (0.76, 2)$, a moderate facility with initial condition $(2.6, 8)$, and
574 a poor and old facility with initial condition $(2.7, 20)$. In both figures, the length and color of an
575 arrow represent the interval between two consecutive inspections and the M&R type (green for
576 do-nothing, yellow for rehabilitation, and red for reconstruction), respectively. The figures show

that inspections are not performed every year. Instead, the gap between two consecutive inspections varies from 1 to 4 years. This indicates the difference between the condition-based and the conventional time-based inspection scheduling methods. Although most inspections do not lead to immediate M&R actions, frequent inspections are still necessary because, if a facility's M&R action is overdue due to the lack of inspection, the ensuing user cost would be huge. Moreover, fewer rehabilitation and reconstruction activities are performed under a lower budget, while the inspection frequencies are similar for the two budget cases. This is consistent with the findings revealed by **Figure 3**. Comparison between the three trajectories in each figure also unveils that the initial pavement condition significantly affects the optimal policy.

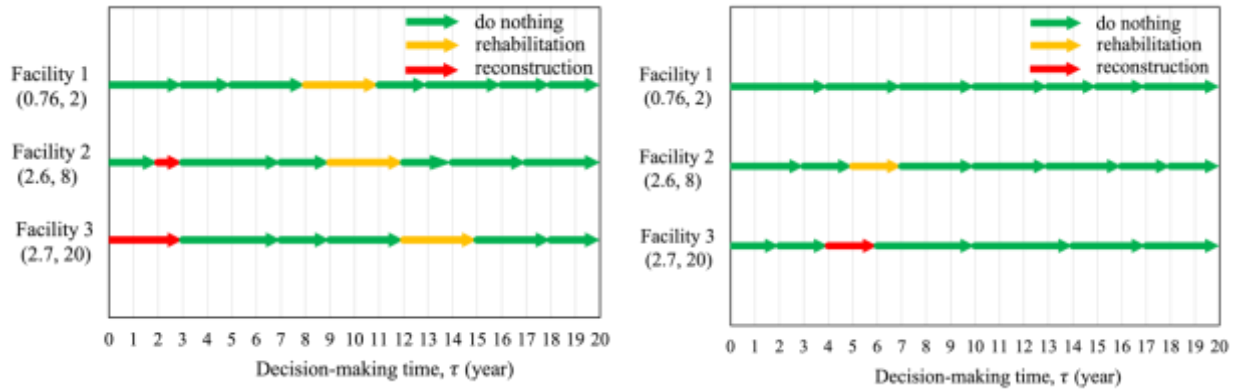

(a) $B = 7 \times 10^5$ \$/year (b) $B = 5 \times 10^5$ \$/year

Figure 4. Realizations of optimal policies.

5.4.3 Convergence of the updating process and its impact on the user cost

We now examine the convergence of deterioration model parameter estimates. The updating trajectories of two parameters, $\hat{\theta}^1$ and $\hat{\theta}^2$, are selected and plotted in **Figures 5a** and **5b**. The two figures present identical systems with an annual budget $B^\tau \equiv B = 6 \times 10^5$ \$/year, $\forall \tau$. The true parameter values are $\theta^1 = 0.04$, $\theta^2 = 930$, as shown by the black dot in each figure. **Figure 5a** uses 100 historical data records before the initial decision-making time $\tau = 0$, while **Figure 5b** uses 300. Each arrow in a trajectory represents five updates, and the cumulative number of updates is displayed near the arrowhead in red.

With 100 historical data records, the initial estimation at $\tau = 0$ gives $(\hat{\theta}^1, \hat{\theta}^2) = (0.051, 835)$, while those estimates are more accurate at $(0.042, 970)$ with 300 historical data

records. This is expected. As more inspections are performed, the parameter estimates quickly approach the ground truth through our model updating process, as illustrated in **Figures 5a** and **5b**. With the same number of updates, the improvement over the initial estimates is greater when the historical dataset is more limited. It is worth noting that during each update, the deterioration model parameters are updated using the inspection data collected from all the inspected facilities.

Finally, we investigate how the model updating process affects the user cost. The same numerical instances as in **Figures 5a** and **5b** are used. For the instance in **Figure 5a**, we compare the total user cost for 20 years with and without model updating. If model updating is performed, the deterioration model will be updated 17 times in 20 years. Results show that the model updating process can reduce the user cost by 10.7%. For the instance in **Figure 5b**, the user cost reduction is 5.9% for a total of 20 years with 16 model updates. This manifests the sizeable benefit of updating the agency's beliefs on pavement deterioration via inspections. The benefit is greater when the initial belief is less accurate (i.e., in the case of **Figure 5a**).

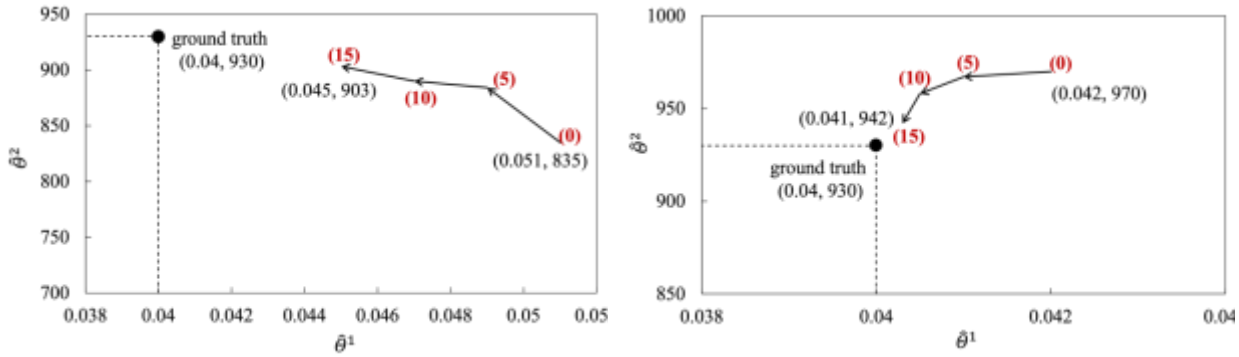

(a) 100 historical data records (b) 300 historical data records

Figure 5. Convergence of the estimated deterioration model parameters.

5.4.4 Benefit of condition-based inspection scheme

To examine the benefit of the condition-based inspection scheme, we compare the optimal total user cost at $\tau = 0$ against that of a benchmark model with a time-based inspection scheme. For conservativeness, the inspection period of each facility is optimized in the benchmark model. The percentage of user cost saving of condition-based inspection is plotted against the budget in **Figure 6**. It reveals that the saving decreases as the budget increases, ranging from 4.3% to 1.9%. Note that although these percentage savings are modest, the dollar values of the savings resulting from the condition-based inspection could be huge, given that poor pavement conditions cost motorists

hundreds of billion of US dollars annually (ASCE, 2017). This manifests the considerable benefit of incorporating a condition-based inspection scheme, especially when the budget is meager.

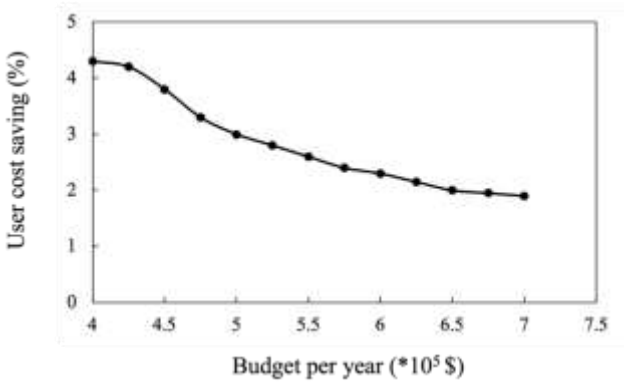

Figure 6. Effect of budget on user cost saving

5.4.5 Sensitivity analysis of unit inspection cost

We still use two annual budget values: (i) $B^{\tau} \equiv B = 7 \times 10^5$ \$/year (**Figure 7a**) and (ii) $B^{\tau} \equiv B = 5 \times 10^6$ \$/year (**Figure 7b**). In each figure, the optimal expected user and agency cost components are plotted against the mean unit inspection cost varying from 3E2 to 2.1E3 \$/km/lane (a seven times increase). For a given mean unit inspection cost $\overline{ci}$, the facility-specific unit inspection cost ci_n is generated from a uniform distribution $U[\overline{ci} - \text{E2}, \overline{ci} + \text{E2}]$.

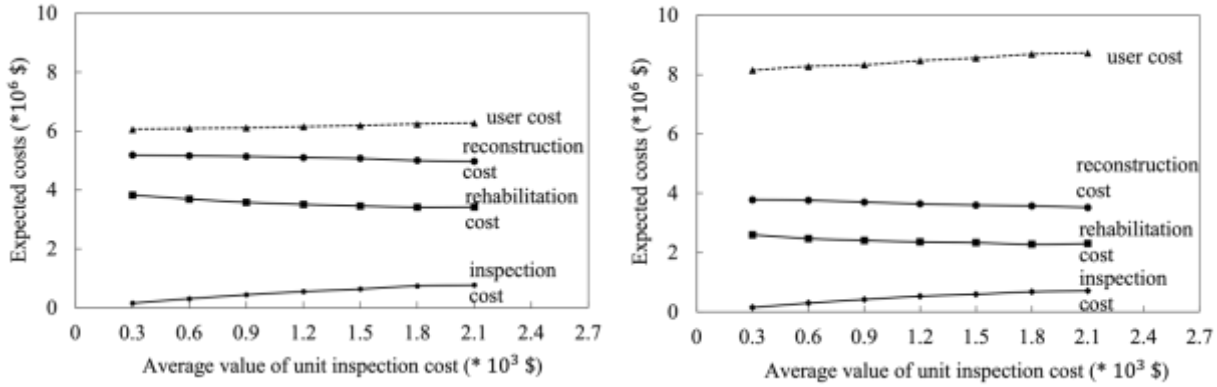

(a) $B = 7 \times 10^5$ \$/year (b) $B = 5 \times 10^5$ \$/year

Figure 7. Effect of the unit inspection cost on cost components

The two figures reveal that all the cost components save for the inspection cost are fairly insensitive to the unit inspection cost. Specifically, rehabilitation and reconstruction costs diminish

as the unit inspection costs grow, indicating that fewer M&R activities are performed due to the increased inspection cost and reduced inspection frequency. As a result, the user cost increases. The slowed model updating process also has an adverse effect on the optimal M&R planning and user cost. The resulting user cost growth is more prominent when the budget is meagerer.

5.4.6 Computational efficiency

We perform numerical experiments for systems consisting of $N = 50$, 100, 150, 200, 250, and 300 facilities. For each N, the average computation time of 20 numerical instances for a one-off optimization at $\tau = 0$ with $T = 20$ years is calculated and plotted in **Figure 8**. The figure exhibits a polynomial relationship between the computational time and the system size.

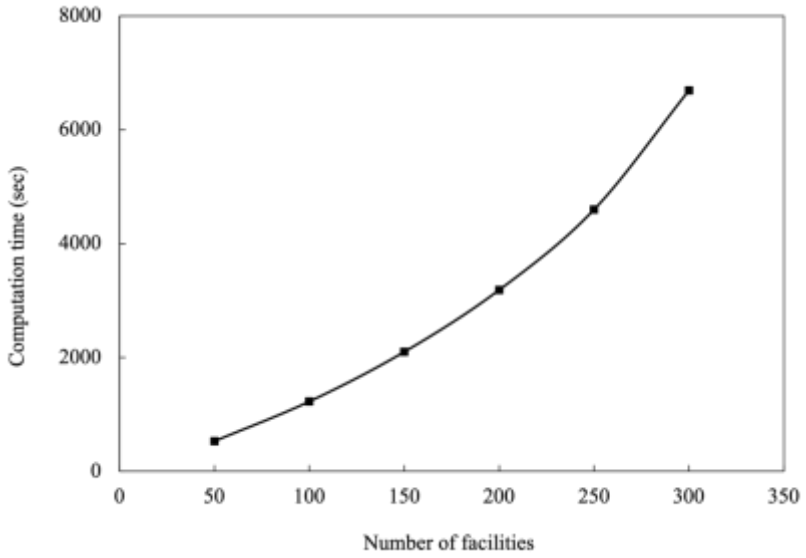

Figure 8. Average computation time for the proposed algorithm

6. CONCLUSIONS

In this paper, we formulate a stochastic model for the joint optimization of inspection and M&R policies for heterogeneous pavement systems under model uncertainties. An algorithm is developed on a rolling-horizon basis. At each time step, the algorithm uses a Lagrange multiplier approach combined with dynamic programming to solve the system-level problem. Meanwhile, we utilize a statistical learning approach for updating the deterioration prediction whenever new inspection data is collected from the pavements.

We summarize the main contributions of our work as follows:

(iii) To our best knowledge, this is the first paper to develop a joint optimization framework of condition-based inspection and M&R activity planning for heterogeneous facilities. This allows the management agency to utilize the limited budget more effectively than the conventional time-based inspection scheme by reducing unnecessary inspections (see Section 5.4.4). The integration of inspection scheduling adds another dimension to the solution space compared to previous studies (e.g., Zhang et al., 2017; Shon and Lee, 2021). Despite the added complexity, the problem can be solved by our proposed approach within a moderate runtime (see Section 5.4.6).

(iv) We are also the first to incorporate belief updates of model uncertainties into the rolling-horizon-based planning framework. This allows the agency to exploit the inspection data timely to understand pavement deterioration better. Numerical results show that the ensuing cost reduction in the long term is substantial (see Section 5.4.3).

(v) Our numerical case studies unveil managerial insights that can enhance agencies' understanding of inspection and M&R planning practices. Examples of these insights include: (a) under an inadequate budget, perform more rehabilitations but fewer reconstructions; and (b) it is beneficial to maintain a certain frequency of inspections even under a highly-limited budget.

Admittedly, our research still has limitations. For example, the network-level impacts of pavement conditions and M&R activities on traffic redistribution and the associated costs (Mack et al., 2018) are not properly modeled in this study. This problem may be addressed by formulating a bi-level program, with the lower level developing the traffic assignment equilibrium and the upper level optimizing the M&R schedules. However, the difficulty lies in how to decompose the system-level problem in this case. Also ignored are the environmental impacts of M&R activities (Mack et al., 2017; Santos et al., 2020), which can be incorporated as either part of the system cost or a constraint.

A specific functional form of the pavement deterioration model may result in prediction biases. Non-parametric models and reinforcement learning techniques can be employed to overcome this shortcoming. Moreover, the brief updates of model uncertainties can be integrated into the optimization framework, resulting in more cost-effective inspection schedules. Lastly, we

ignored the uncertainty in imperfect inspection measurements, which also has significant lifecycle cost implications (Shon et al., 2022). The above issues will be addressed in our future work.

ACKNOWLEDGMENTS

The Research Grant Council of Hong Kong supported this work under the General Research Fund (Project Number 15280116). Natural Science Foundation of China (Project Number 72101115), Natural Science Foundation of Jiangsu (Project Number BK20210316), and National Research Foundation of Korea (NRF) grant funded by the Korea government (MSIT) (No. 2020R1C1C1005034) supported this work.

AUTHOR CONTRIBUTION STATEMENT

Le Zhang: Conceptualization, Methodology, Software, Formal analysis, Investigation, Data Curation, Writing - Original Draft, Visualization, Funding acquisition

Weihua Gu: Conceptualization, Validation, Resources, Writing - Review & Editing, Supervision, Project administration, Funding acquisition

Young-ji Byon: Validation, Writing - Review & Editing

Jinwoo Lee: Conceptualization, Methodology, Formal analysis, Writing - Original Draft, Project administration

Appendix A. List of notations

TABLE A1. List of notations.

Notation	Description
Sets and Indices	
N	set of facilities
n	facility index
$\mathbb{S}_n$	set of all possible conditions for facility n
s_n	condition index of facility n
$\mathbb{M}_n$	set of M&R activities on facility n
h	facility age
r	roughness level index
T	planning horizon
τ	current time index
t	future time index
t^I	time stage for making the inspection decision
t^{II}	time stage for making the M&R action decision
t^{III}	time stage for deterioration (after the M&R activity has taken place)
Decision variables	
$\boldsymbol{x}_n(t^I) \in \{0,1\}$	equals one if an inspection is conducted at t^I on facility n, and zero otherwise

$\boldsymbol{x}(t^I)$	set of $\boldsymbol{x}_n(t^I)$, $\forall n$
$\Delta_n(t)$	time gap between time t and the time of the next inspection if $\boldsymbol{x}_n(t^I) = 1$ for facility n
$\boldsymbol{y}_n(t^{II})$	M&R activity decision applied on facility n at t^{II}
$\boldsymbol{\varpi}_{n,t}$	rehabilitation intensity of facility n at t
$\boldsymbol{\chi}^1_{n,t} \in \{0,1\}$	equals one if rehabilitation is conducted at t on facility n, and zero otherwise
$\boldsymbol{\chi}^2_{n,t} \in \{0,1\}$	equals one if reconstruction is conducted at t on facility n, and zero otherwise
Parameters and other variables	
B^τ	annual average long-term budget known at time τ
d	true deterioration model
$\hat{d}^\tau$	belief of the deterioration model, the best estimate of deterioration model available at time τ
$\hat{p}^\tau$	belief of the current condition before inspection, the set of probabilities of the condition of facility n at t^I estimated by the belief of the deterioration model available at time τ
$S_n(t^I)$	true condition of facility n at t^I
$\hat{S}_n(t^I)$	estimated condition of facility n at t^I
$S_n(t^{II})$	true condition of facility n at t^{II} if an inspection was conducted at t^I
$\tilde{S}_n(t^{II})$	observed condition of facility n at t^{II} if an inspection was conducted at t^I
$S_n(t^{III})$	improved condition of facility n at t^{III} after an M&R activity
$R_n(t)$	roughness level of facility n at t
r^{new}	best achievable roughness level
r^{max}	upper bound of pavement roughness level
l_n	traffic loading of facility n
SN_n	structural number of facility n
$Age_n(t)$	age of facility n at t since its construction or the last reconstruction
$\xi^\tau(\cdot)$	deterioration process at decision time point τ
X_n^τ	set of facility-specific influential factors in model $\xi^\tau(\cdot)$
$\hat{\theta}^\tau$	set of systemwide parameters in model $\xi^\tau(\cdot)$
$\hat{\varepsilon}^\tau$	set of systemwide model uncertainties in model $\xi^\tau(\cdot)$
$\hat{\phi}_n^\tau$	set of facility-specific model uncertainties in model $\xi^\tau(\cdot)$
$J_{[0,T]}$	total discounted user cost over planning horizon $[0,T]$
$\hat{J}_{[0,T]}$	predicted total discounted user cost over the planning horizon $[0,T]$
$\hat{J}_{n,[0,T]}$	predicted discounted user cost of facility n over planning horizon $[0,T]$
$\hat{A}_{[0,T]}$	predicted total discounted agency cost over the planning horizon $[0,T]$
$\hat{A}_{n[0,T]}$	predicted discounted agency cost of facility n over planning horizon $[0,T]$
$H_{n,[0,T]}$	defined as $\hat{J}_{n,[0,T]}(x_n, y_n) + \lambda \cdot \hat{A}_{n,[0,T]}(x_n, y_n)$
u	user cost associated with pavement serviceability
u_n	user cost of facility n associated with its serviceability
w	user cost resulting from work-zone impact of M&R activities
w_n	user cost of facility n resulting from work-zone impact of its M&R activities
α	discounting factor
ci_n	unit inspection cost for facility n
$cm_n(\cdot)$	M&R cost for facility n
$\boldsymbol{\lambda}$	Lagrange multiplier
$TC(\cdot)$	terminal cost
$\ell_n(t)$	number of basis functions for facility n in period t in the ADP framework
$c_{n,1}, c_{n,2}, \gamma_{n,1}, \gamma_{n,2}, z_{n,1}, z_{n,2}$, and β_n	cost coefficients for facility n
g^1, g^2, and g^3	coefficients for the rehabilitation effectiveness model

Appendix B. Approximate dynamic programming method for the facility-level problem

For a better tradeoff between the solution quality and computational tractability, we solve the POMDP problem (**Equations (14-16)**) using ADP. The details are outlined as follows: an approximation of the value function is presented in Section B.1; the learning process of updating the approximate value function based on the simulated sample path is furnished in Section B.2; and finally, the tradeoff between exploration and exploitation is discussed in Section B.3.

B.1 Value function approximation

We approximate the value function as a linear combination of basis functions shown in **Equation (B1)**. This technique was commonly used in the ADP literature (Sutton and Barto, 1998; Kuhn, 2010; Medury and Madanat, 2013):

$$\tilde{Q}_n^t(S_n(t^{II}), \boldsymbol{y}_n(t^{II}), \Delta_n(t)|\boldsymbol{\lambda}) = \sum_{i=1}^{\ell_n(t)} \rho_n^i(t|\lambda) \cdot \xi_n^i(S_n(t^{II}), \boldsymbol{y}_n(t^{II}), \Delta_n(t)), \tag{B1}$$

where $\tilde{Q}_n^t(S_n(t^{II}), \boldsymbol{y}_n(t^{II}), \Delta_n(t)|\boldsymbol{\lambda})$ is an approximation of the expected cost-to-go from period $t + \Delta_n(t)$ to $T - 1$ when M&R action $\boldsymbol{y}_n(t^{II})$ and inspection $\boldsymbol{x}_n((t + \Delta_n(t))^I)$ are applied to facility n with state $S_n(t^{II})$, termed as the Q-function; $\xi_n^i(S_n(t^{II}), \boldsymbol{y}_n(t^{II}), \Delta_n(t))$ is a basic function capturing important attributes of facility conditions, available M&R actions, and inspection options, termed the Q-factor; $\rho_n^i(t|\boldsymbol{\lambda})$ is the weighting factor associated with basic function $\xi_n^i(S_n(t^{II}), \boldsymbol{y}_n(t^{II}), \Delta_n(t))$, which will be refined within the ADP framework; and $\ell_n(t)$ is the total number of basic functions for facility n during period t.

Given the Q-function, $\tilde{Q}_n^t(S_n(t^{II}), \boldsymbol{y}_n(t^{II}), \Delta_n(t)|\boldsymbol{\lambda})$, the optimal M&R and inspection actions at period t can be obtained as follows:

$$\min_{\boldsymbol{y}_n(t^{II}), \Delta_n(t)} \left\{ R_n(S_n(t^{II}), \boldsymbol{y}_n(t^{II}), \Delta_n(t)) + \tilde{Q}_n^t(S_n(t^{II}), \boldsymbol{y}_n(t^{II}), \Delta_n(t)|\boldsymbol{\lambda}) \right\}, \tag{B2}$$

where

$$R_n(S_n(t^{II}), \boldsymbol{y}_n(t^{II}), \Delta_n(t)) = \boldsymbol{\lambda} cm_n\left(\boldsymbol{y}_n(t^{II})\right) + u_n\left(f\left(S_n(t^{II}), \boldsymbol{y}_n(t^{II})\right)\right) +$$
$$w_n\left(S_n(t^{II}), \boldsymbol{y}_n(t^{II})\right) + \sum_{\mu=1}^{\Delta_n(t)-1} \alpha^{\mu} \underset{S_n(t+\mu)^I}{E}[u_n(S_n((t+\mu)^I))] + \boldsymbol{\lambda} \alpha^{\Delta_n(t)} \cdot ci_n$$

is termed the step reward. **Equation (B2)** shows that once we know the estimated Q-function, the optimal management actions can be obtained directly, where the step reward $R_n(S_n(t^{II}), \boldsymbol{y}_n(t^{II}), \Delta_{\boldsymbol{n}}(t))$ can be obtained by Monte Carlo simulation. This can largely reduce the complexity caused by computing the expectation of future cost, especially when the outcome space is large.

B.2 Updating the approximate value function

At the k-th ADP iteration, denote the current condition state of facility n by $S_{n,k}(t^{II})$. The optimal action $\{\overline{\boldsymbol{y}}_{n,k}(t^{II}), \bar{\Delta}_{n,k}(t)\}$ is selected according to **Equation (B3)**:

$$\{\overline{\boldsymbol{y}}_{n,k}(t^{II}), \bar{\Delta}_{n,k}(t)\} = \underset{\boldsymbol{y}_{n,k}(t^{II}), \Delta_{n,k}(t)}{\operatorname{argmin}} \{R_n(S_{n,k}(t^{II}), \boldsymbol{y}_{n,k}(t^{II}), \Delta_{n,k}(t)) + \tilde{Q}^t_{n,k-1}(S_{n,k}(t^{II}), \boldsymbol{y}_{n,k}(t^{II}), \Delta_{n,k}(t)|\boldsymbol{\lambda})\}, \quad \text{(B3)}$$

where the Q-function $\tilde{Q}^t_{n,k-1}(S_{n,k}(t^{II}), \boldsymbol{y}_{n,k}(t^{II}), \Delta_{n,k}(t)|\boldsymbol{\lambda})$ is obtained during the previous iteration. Once action $\overline{\boldsymbol{y}}_{n,k}(t^{II})$ has been performed and $\bar{\Delta}_{n,k}(t)$ is determined, a sample realization of the future state $S_{n,k}(t + \bar{\Delta}_{n,k}(t))$ is generated by a Monte Carlo simulation procedure following the stochastic deterioration process, $\hat{p}^{\tau}(\cdot)$.

Once a sample state of period $t + \bar{\Delta}_{n,k}(t)$ is ascertained, the optimal action for period $t + \bar{\Delta}_{n,k}(t)$ can be selected by repeatedly applying **Equation (B3)**. The procedure is repeated until the end of the planning horizon. Then we get a sequence of state-action pairs:

$$[(S_{n,k}(t_1^{II}), \overline{\boldsymbol{y}}_{n,k}(t_1^{II}), \bar{\Delta}_{n,k}(t_1)), (S_{n,k}(t_2^{II}), \overline{\boldsymbol{y}}_{n,k}(t_2^{II}), \bar{\Delta}_{n,k}(t_2)), \cdots, (S_{n,k}(t_z^{II}), \overline{\boldsymbol{y}}_{n,k}(t_z^{II}), \bar{\Delta}_{n,k}(t_z)), S_{n,k}(t_{z+1}^{II})], \quad \text{(B4)}$$

where $t_{i+1}^{II} - t_i^{II} = \bar{\Delta}_{n,k}(t_i), 0 \le i \le z-1, t_1 = 0, t_{z+1}^{II} = T$ and $t_{z+1}^{II} - t_z^{II} \le \bar{\Delta}_{n,k}(t_z)$.

The state-action sequence **(B4)** is termed a *sample path*. We will repeat the above process for K iterations. We always assume that the current Q-function is the best estimate of future cost-to-go at each iteration.

We next use the TD($\bar{\omega}$) method to update the parameters of the approximate value function backward recursively based on the realized sample path. The error term is defined as:

$$\begin{aligned}\Lambda_{n,k}(t_i^{II}) = \sum_{\tau=i}^{z} (\alpha\bar{\omega})^{t_\tau - t_i} (R_n\left(S_{n,k}(t_{\tau+1}^{II}), \bar{\boldsymbol{y}}_{n,k}(t_{\tau+1}^{II}), \bar{\Delta}_{n,k}(t_{\tau+1})\right) \\ +\alpha\tilde{Q}_{n,k-1}^{t_{\tau+1}}\left(S_{n,k}(t_{\tau+1}^{II}), \bar{\boldsymbol{y}}_{n,k}(t_{\tau+1}^{II}), \bar{\Delta}_{n,k}(t_{\tau+1})|\boldsymbol{\lambda}\right) \\ -\tilde{Q}_{n,k-1}^{t_\tau}\left(S_{n,k}(t_\tau^{II}), \bar{\boldsymbol{y}}_{n,k}(t_\tau^{II}), \bar{\Delta}_{n,k}(t_\tau)|\boldsymbol{\lambda}\right)), \qquad \forall i \in \{1,2,\cdots,z\}\end{aligned} \tag{B5}$$

where $\bar{\omega} \in [0,1]$ is the artificial discount factor. Once the temporal difference error $\Lambda_{n,k}(t)$ is calculated for a given period t in the k-th ADP iteration, the weighting factors can be updated using a stochastic gradient algorithm:

For $i \in \{1,2,\cdots,z\}, j \in \{1,2,\cdots,\ell_n(t)\}$

$$\rho_{n,k}^{j}(t_i|\boldsymbol{\lambda}) = \rho_{n,k-1}^{j}(t_i|\boldsymbol{\lambda}) + \gamma_k \frac{\partial \vartheta_{n,k}(t)}{\partial \rho_n^j(t|\lambda)} \cdot \Lambda_{n,k}(t_i^{II}) \tag{B6}$$

where

$$\vartheta_{n,k}(t) = R_n\left(S_{n,k}(t^{II}), \boldsymbol{y}_{n,k}(t^{II}), \Delta_{n,k}(t)\right) + \tilde{Q}_{n,k-1}^{t}\left(S_{n,k}(t^{II}), \boldsymbol{y}_{n,k}(t^{II}), \Delta_{n,k}(t)|\boldsymbol{\lambda}\right)$$

The following basic conditions should be satisfied for the step-size parameter γ_k to guarantee convergence:

$$\gamma_k \geq 0, \forall k = 1,2,\cdots, \tag{B7}$$

$$\sum_{k=1}^{\infty} \gamma_k = \infty, \tag{B8}$$

$$\sum_{k=1}^{\infty} \gamma_k^2 < \infty. \tag{B9}$$

The proposed ADP framework for solving the facility-level problem over a finite time horizon is summarized as follows:

Algorithm B.1

Step 0: Initialization:

Step 0.1: Initialize $\tilde{Q}_{n,0}^{t}\left(S_{n,0}(t^{II}), \boldsymbol{y}_{n,0}(t^{II}), \Delta t|\boldsymbol{\lambda}\right),\ \forall S_{n,0}(t^{II}) \in \mathbb{S}_n, \boldsymbol{y}_{n,0}(t^{II}) \in \mathbb{M}_n, t = 0, \cdots T-1$.

Step 0.2: Choose an initial state $S_{n,0}(0^{II})$.

Step 1: Do for $k = 1,2, \cdots K$ (record the index of iteration in the ADP framework):

Step 1.2: Initialize $z = 0, t_1 = 0$ and Do for $t_{z+1} < T$:

Step 1.2.1: Set $z \leftarrow z + 1$.

Step 1.2.2: Solve $\hat{\vartheta}_{n,k}(t_z) = \min_{\boldsymbol{y}_{n,k}(t_z^{II}), \Delta_{n,k}(t_z)} R_n\left(S_{n,k}(t_z^{II}), \boldsymbol{y}_{n,k}(t_z^{II}), \Delta_{n,k}(t_z)\right) + \tilde{Q}_{n,k-1}^{t}\left(S_{n,k}(t_z^{II}), \boldsymbol{y}_{n,k}(t_z^{II}), \Delta_{n,k}(t_z)|\boldsymbol{\lambda}\right)$, and denote $\left\{\overline{\boldsymbol{y}}_{n,k}(t_z^{II}), \bar{\Delta}_{n,k}(t_z)\right\}$ the corresponding optimal solution.

Step 1.2.3: Get a sample realization of the future state $S_{n,k}\left(t_z + \bar{\Delta}_{n,k}(t_z)\right)$.

Step 1.2.4: Set $t_{z+1} \leftarrow \min\left\{t_z + \bar{\Delta}_{n,k}(t_z), T\right\}$.

Step 1.3: Initialize $\Lambda_{n,k}(t_z^{II}) = 0$, $\hat{\vartheta}_{n,k}(T) \leftarrow TC(S_n(T)|\boldsymbol{\lambda})$.

Step 1.4: Do for $i = z, z-1, \cdots, 1$:

Step 1.4.1: Set $\varsigma_n(t_i) \leftarrow \hat{\vartheta}_{n,k}(t_{i+1}) - \tilde{Q}_{n,k-1}^{t_i}\left(\left(S_{n,k}(t_i^{II}), \overline{\boldsymbol{y}}_{n,k}(t_i^{II}), \bar{\Delta}_{n,k}(t_i)|\boldsymbol{\lambda}\right)\right)$.

Step 1.4.2: Set $\Lambda_{n,k}(t_i^{II}) \leftarrow \Lambda_{n,k}(t_i^{II}) + \varsigma_n(t_i)$.

Step 1.4.3: Update $\rho_{n,k}^{j}(t_i|\boldsymbol{\lambda}) \leftarrow \rho_{n,k}^{j}(t_i|\boldsymbol{\lambda}) + \gamma_k \frac{\partial \vartheta_{n,k}(t)}{\partial \rho_n^j(t|\boldsymbol{\lambda})} \cdot \Lambda_{n,k}(t_i^{II})$ for s $j \in \{1,2, \cdots, \ell_n(t)\}$.

Step 1.4.4: Set $\Lambda_{n,k}(t_{i-1}^{II}) \leftarrow \alpha\bar{\omega}\Lambda_{n,k}(t_i^{II})$ for $i > 1$.

B.3 Exploration versus exploitation

One of the challenges in ADP is the tradeoff between exploration and exploitation. The decision-maker must exploit what is already known to obtain the lowest cost, but she also needs to explore in order to obtain more information. In this paper, an ε-greedy policy is employed. With a small probability ε, the policy will randomly select the maintenance action among all the options, independent of the action-value estimates. The policy is formulated as follows:

For $k = 1,2, \cdots K, t = 1,2, \cdots T,$ (B10)

$$Prob\left(\boldsymbol{y}_{n,k}(t^{II})\middle|S_{n,k}(t^{II})\right)=\begin{cases}1-\varepsilon+\frac{\varepsilon}{\mathbb{A}}, & \text{if } \boldsymbol{y}_{n,k}(t^{II})=\bar{\boldsymbol{y}}_{n,k}(t^{II}),\Delta_{n,k}(t)=\bar{\Delta}_{n,k}(t)\\ \frac{\varepsilon}{\mathbb{A}}, & \text{otherwise}\end{cases},$$

$$\forall S_{n,k}(t^{II})\in\mathbb{S}_n,\boldsymbol{y}_{n,k}(t^{II})\in\mathbb{M}_n$$

where $\mathbb{A}$ denotes the size of the available action set.

APPENDIX C. Updating the Lagrange multiplier

In the following numerical algorithm, the Lagrange multiplier in the k-th iteration is denoted by λ^k. The algorithm is based on the assumption that the Lagrange function $L^*(x,y|\lambda)$ is a pseudo-convex envelope with respect to λ (Lee et al., 2016).

Algorithm C.1

Step 0: Initialization:

Step 0.1: Initialize $\boldsymbol{\lambda}^0=0$ and find $\{\boldsymbol{x}^0(0^I),\boldsymbol{y}^0(0^{II})\}=\{\boldsymbol{x}^*(0^I),\boldsymbol{y}^*(0^{II})|\boldsymbol{\lambda}^0\}$.

Step 0.2: If $\{\boldsymbol{x}^0(0^I),\boldsymbol{y}^0(0^{II})\}$ satisfies the budget constraint, then stop. Otherwise, go to Step 1.

Step 1: Randomly select $\boldsymbol{\lambda}^1>0$ and find $\{\boldsymbol{x}^1(0^I),\boldsymbol{y}^1(0^{II})\}=\{\boldsymbol{x}^*(0^I),\boldsymbol{y}^*(0^{II})|\boldsymbol{\lambda}^1\}$; set $k=1$.

Step 2: If the budget constraint is not satisfied, do the following:

Step 2.1: Set $k\leftarrow k+1$.

Step 2.2: Update $\boldsymbol{\lambda}^k$ using the gradient approximation method:

$\boldsymbol{\lambda}^k=\boldsymbol{\lambda}^{k-1}-\bar{\alpha}^{k-1}\cdot\varrho^{k-1}/(\boldsymbol{\lambda}^{k-1}-\boldsymbol{\lambda}^{k-2})$, where

$\varrho^{k-1}=L(\boldsymbol{x}^{k-1}(0^I),\boldsymbol{y}^{k-1}(0^{II}))-L\left(\boldsymbol{x}^{k-2}(0^I),\boldsymbol{y}^{k-2}(0^{II})\right)$ and $\bar{\alpha}_{k-1}$ is a positive step size.

Step 2.3: Find $\{\boldsymbol{x}^k(0^I),\boldsymbol{y}^k(0^{II})\}=\{\boldsymbol{x}^*(0^I),\boldsymbol{y}^*(0^{II})|\boldsymbol{\lambda}^k\}$.

Appendix D. Updating deterioration model

We assume that the true error term ε_τ follows a normal distribution denoted by $N(0,\sigma_\tau^2)$. The data associated with a new inspection are presented in the form of $\left(r_{before}^{d,n}(t^{III}),\ r_{after}^{d,n}(t'^{II}),\ h_{before}^{d,n}(t^{III}),\ h_{after}^{d,n}(t'^{II})\right)$, where t and t' denote the times of two consecutive inspections on

facility n, $t < t'$; $r_{before}^{d,n}(t^{III})$ and $r_{after}^{d,n}(t'^{II})$ denote the roughness levels of facility n at time t^{III} and t'^{II}, respectively; $h_{before}^{d,n}$ and $h_{after}^{d,n}$ are the facility ages at t^{III} and t'^{II}, respectively; and d is the data index. In what follows, notation $\left(r_{before}^{d,n}(t^{III}),\ r_{after}^{d,n}(t'^{II}),\ h_{before}^{d,n}(t^{III}),\ h_{after}^{d,n}(t'^{II})\right)$ is simplified as $\left(r_{before}^{d,n},\ r_{after}^{d,n},\ h_{before}^{d,n},\ h_{after}^{d,n}\right)$. As more inspections are performed, the data size increases, and so does the accuracy of our deterioration model. We denote D the number of data records available by time τ. Since the error terms are independent and identically distributed random variables, we can derive the following:

$$\left(r_{after}^{d,n} - r_{before}^{d,n} e^{\Theta_\tau^1\left(h_{after}^{d,n} - h_{before}^{d,n}\right)} - \Theta_\tau^2 l_n \cdot \left(h_{after}^{d,n} - h_{before}^{d,n}\right) \cdot (1 + SN_n)^{\Theta_\tau^3} e^{\Theta_\tau^1 \cdot h_{after}^{d,n}}\right) \sim N\left(0, \left(h_{after}^{d,n} - h_{before}^{d,n}\right)\sigma_\tau^2\right), \tag{D1}$$

i.e.,

$$\frac{1}{\sqrt{h_{after}^{d,n} - h_{before}^{d,n}}}\left(r_{after}^{d,n} - r_{before}^{d,n} e^{\Theta_\tau^1 (h_{after}^{d,n} - h_{before}^{d,n})} - \Theta_\tau^2 l_n \cdot \left(h_{after}^{d,n} - h_{before}^{d,n}\right) \cdot (1 + SN_n)^{\Theta_\tau^3} e^{\Theta_\tau^1 \cdot h_{after}^{d,n}}\right) \sim N(0, \sigma_\tau^2). \tag{D2}$$

We define:

$$\bar{G}\left(r_{before}^{d,n}, r_{after}^{d,n}, h_{before}^{d,n}, h_{after}^{d,n}\right) = \frac{1}{\sqrt{h_{after}^{d,n} - h_{before}^{d,n}}}\left(r_{after}^{d,n} - r_{before}^{d,n} e^{\Theta_\tau^1\left(h_{after}^{d,n} - h_{before}^{d,n}\right)} - \Theta_\tau^2 l_n \cdot (h_{after}^{d,n} - h_{before}^{d,n}) \cdot (1 + SN_n)^{\Theta_\tau^3} e^{\Theta_\tau^1 \cdot h_{after}^{d,n}}\right). \tag{D3}$$

Then the likelihood function is:

$$\bar{L}(\Theta_\tau^1, \Theta_\tau^2, \Theta_\tau^3, \sigma_\tau^2) = \prod_{d=1}^{D} \rho\left(\bar{G}\left(r_{before}^{d,n}, r_{after}^{d,n}, h_{before}^{d,n}, h_{after}^{d,n}\right)\right), \tag{D4}$$

where $\rho(\cdot)$ denotes the probability density function of a normal distribution with zero mean and variance of σ_τ^2.

We define:

$$\bar{l}(\Theta_\tau^1, \Theta_\tau^2, \Theta_\tau^3, \sigma_\tau^2) = \log \bar{L}(\Theta_\tau^1, \Theta_\tau^2, \Theta_\tau^3, \sigma_\tau^2)$$
$$= -\frac{D}{2}\log 2\pi - \frac{D}{2}\log \sigma_\tau^2 - \frac{\sum_{d=1}^{D} \bar{G}^2\left(r_{before}^{d,n}, r_{after}^{d,n}, h_{before}^{d,n}, h_{after}^{d,n}\right)}{2\sigma_\tau^2}. \quad \text{(D5)}$$

The values of parameters $\Theta_\tau^1, \Theta_\tau^2, \Theta_\tau^3, \sigma_\tau$ are updated by solving the following equations:

$$\frac{\partial \bar{l}}{\partial \Theta_\tau^i} = -\frac{1}{\sigma_\tau^2}\sum_{d=1}^{D} \bar{G}\left(r_{before}^{d,n}, r_{after}^{d,n}, h_{before}^{d,n}, h_{after}^{d,n}\right) \cdot \frac{\partial \bar{G}\left(r_{before}^{d,n}, r_{after}^{d,n}, h_{before}^{d,n}, h_{after}^{d,n}\right)}{\partial \Theta_t^i} = 0, \forall i = 1, 2, 3, \quad \text{(D6)}$$

$$\frac{\partial \bar{l}}{\partial \sigma_\tau} = -\frac{D}{\sigma_\tau} + \frac{\sum_{d=1}^{D} \bar{G}^2\left(r_{before}^{d,n}, r_{after}^{d,n}, h_{before}^{d,n}, h_{after}^{d,n}\right)}{\sigma_\tau^3} = 0. \quad \text{(D7)}$$

REFERENCES

ASCE, 2017. 2017 infrastructure report card: A comprehensive assessment of America's Infrastructure. (accessed on May 2, 2017). American Society of Civil Engineers, Reston, Virginia. http://www.infrastructurereportcard.org/wp-content/uploads/2016/10/2017-Infrastructure-Report-Card.pdf

Beutler, F., Ross, K., 1985. Optimal policies for controlled Markov chains with a constraint. Operations Research, 55(6), 1120.

Chu, J., Chen, Y., 2012. Optimal threshold-based network-level transportation infrastructure lifecycle management with heterogeneous maintenance actions. Transportation Research Part B: Methodological, 46(9), 1123-1143.

Chu, J.C., Huang, K.H., 2018. Mathematical programming framework for modeling and comparing network-level pavement maintenance strategies. Transportation Research Part B: Methodological, 109, 1-25.

873 Donev, V., Hoffmann, M., 2020. Optimization of pavement maintenance and rehabilitation
874 activities, timing and work zones for short survey sections and multiple distress types.
875 International Journal of Pavement Engineering, 21 (5), 583-607.
876 Durango-Cohen, P., Madanat, S., 2002. Optimal maintenance and repair policies in infrastructure
877 management under uncertain facility deterioration rates: an adaptive control approach.
878 Transportation Research Part A: Policy and Practice, 36(9), 763-778.
879 Durango-Cohen, P., 2004. Maintenance and repair decision making for infrastructure facilities
880 without a deterioration model. Journal of Infrastructure Systems, 10(1), 1-8.
881 Feinberg, E., Shwartz, A., 1996. Constrained discounted dynamic programming. Mathematics of
882 Operations Research, 21(4), 922-945.
883 Fernandez, J.E., Friesz, T.L., 1981. Influence of demand-quality interrelationships on optimal
884 policies for stage construction of transportation facilities. Transportation Science, 15(1), 16-
885 31.
886 France-Mensah, J., O'Brien, W. J., 2019a. Impact of multiple highway funding categories and
887 project eligibility restrictions on pavement performance. Journal of Infrastructure Systems,
888 25(1), 04018037.
889 France-Mensah, J., O'Brien, W. J., 2019b. Developing a sustainable pavement management plan:
890 tradeoffs in road condition, user costs, and greenhouse gas emissions. Journal of Management
891 in Engineering, 35(3), 04019005.
892 Friesz, T.L., Fernandez, J.E., 1979. A model of optimal transport maintenance with demand
893 responsiveness. Transportation Research Part B: Methodological, 13(4), 317-339.
894 Gu, W., Ouyang, Y., Madanat, S., 2012. Joint optimization of pavement maintenance and
895 resurfacing planning. Transportation Research Part B: Methodological, 46(4), 511-519.
896 Islam, S., Buttlar, W. G., 2012. Effect of pavement roughness on user costs.Transportation research
897 record, 2285(1), 47-55.
898 Lee, J., Madanat, S., 2015. A joint bottom-up solution methodology for system-level pavement
899 rehabilitation and reconstruction. Transportation Research Part B: Methodological, 78, 106-
900 122.
901 Lee, J., Madanat, S., Reger, D., 2016. Pavement systems reconstruction and resurfacing policies
902 for minimization of lifecycle costs under greenhouse gas emissions constraints.
903 Transportation Research Part B: Methodological, 93, 618-630.

Levenberg, E., Miller-Hooks, E., Asadabadi, A., Faturechi, R., 2016. Resilience of networked infrastructure with evolving component conditions: pavement network application. Journal of Computing in Civil Engineering, 31(3), 04016060.

Mack, J., Cheng, L., Li, D., 2018. Road maintenance optimization model based on dynamic programming in urban traffic network. Journal of Advanced Transportation, 2018.

Mack, J.W., Akbarian, M., Ulm, F.J., Louhghalam, A., 2017. Pavement-vehicle interaction research at the MIT concrete sustainability hub. International Conference on Highway Pavements and Airfield Technology.

Madanat, S., 1993. Incorporating inspection decisions in pavement management. Transportation Research Part B: Methodological, 27(6), 425-438.

Madanat, S., Park, S., Kuhn, K., 2006. Adaptive optimization and systematic probing of infrastructure system maintenance policies under model uncertainty. Journal of Infrastructure Systems, 12(3), 192-198.

Memarzadeh, M., Pozzi, M., Kolter, J.Z., 2016. Hierarchical modeling of systems with similar components: A framework for adaptive monitoring and control. Reliability Engineering & System Safety, 153, 159-169.

Naseri, H., Fani, A., Golroo, A., 2020. Toward equity in large-scale network-level pavement maintenance and rehabilitation scheduling using water cycle and genetic algorithms. International Journal of Pavement Engineering, 1-13.

Ohlmann, J., Bean, J., 2009. Resource-constrained management of heterogeneous assets with stochastic deterioration. European Journal of Operational Research, 199(1), 198-208.

Ouyang, Y., Madanat, S., 2006. An analytical solution for the finite-horizon pavement resurfacing planning problem. Transportation Research Part B: Methodological, 40(9), 767-778.

Ouyang, Y., 2007. Pavement resurfacing planning for highway networks: parametric policy iteration approach. Journal of Infrastructure Systems, 13(1), 65-71.

Papakonstantinou, K.G., Andriotis, C.P., Shinozuka, M., 2018. POMDP and MOMDP solutions for structural lifecycle cost minimization under partial and mixed observability. Structure and Infrastructure Engineering, 14(7), 869-882.

Papakonstantinou, K.G., Shinozuka, M., 2014a. Planning structural inspection and maintenance policies via dynamic programming and Markov processes. Part I: Theory. Reliability Engineering & System Safety, 130, 202-213.

Papakonstantinou, K.G., Shinozuka, M., 2014b. Planning structural inspection and maintenance policies via dynamic programming and Markov processes. Part II: POMDP implementation. Reliability Engineering & System Safety, 130, 214-224.

Paterson, W.D., 1990. Quantifying the effectiveness of pavement maintenance and rehabilitation. In Road Engineering Association of Asia and Australasia (REAAA), Conference, 6th, 1990, Kuala Lumpur, Malaysia.

Qiao, Y., Fricker, J.D., Labi, S., Sinha, K.C., 2017. Strategic scheduling of infrastructure repair and maintenance: volume 3—developing condition-based triggers for pavement maintenance, rehabilitation, and replacement treatments.

Richmond, C., Achilles, F., Adey, B.T., 2018. Approximating an analytic solution for the optimal design of asphalt pavement: limited example. Journal of Transportation Engineering, Part B: Pavements, 144(4), 04018045.

Ross, K., Varadarajan, R., 1989. Markov decision processes with sample path constraints: the communicating case. Operations Research, 37(5), 780-790.

Santos, J., Torres-Machi, C., Morillas, S., Cerezo, V., 2020. A fuzzy logic expert system for selecting optimal and sustainable life cycle maintenance and rehabilitation strategies for road pavements. International Journal of Pavement Engineering, 1-13.

Schöbi, R., Chatzi, E.N., 2016. Maintenance planning using continuous-state partially observable Markov decision processes and non-linear action models. Structure and Infrastructure Engineering, 12(8), 977-994.

Shi, Y., Xiang, Y., Xiao, H., Xing, L., 2020. Joint optimization of budget allocation and maintenance planning of multi-facility transportation infrastructure system. European Journal of Operational Research, 288 (2), 382-393.

Shon, H. and Lee, J., 2021. Integrating multi-scale inspection, maintenance, rehabilitation, and reconstruction decisions into system-level pavement management systems. Transportation Research Part C: Emerging Technologies, 131, p.103328.

Shon, H., Cho, C., Byon, Y. and Lee, J., 2022. Initial concept of autonomously monitored pavement management systems and its potential benefits. Presented at Transportation Research Board 101st Annual Meeting.

964 Swei, O., Gregory, J., Kirchain, R., 2017. Construction cost estimation: A parametric approach for
965 better estimates of expected cost and variation. Transportation Research Part B:
966 Methodological, 101, 295-305.
967 Swei, O., Gregory, J., Kirchain, R., 2018. Does pavement degradation follow a random walk with
968 drift? Evidence from variance ratio tests for pavement roughness. Journal of Infrastructure
969 Systems, 24(4), 04018027.
970 Thompson, P.D., Small, E.P., Johnson, M., Marshall, A.R., 1998. The Pontis bridge management
971 system. Structural Engineering International, 8(4), 303-308.
972 Torres-Machí, C., Chamorro, A., Videla, C., Pellicer, E., Yepes, V., 2014. An iterative approach for
973 the optimization of pavement maintenance management at the network level. The Scientific
974 World Journal, 2, 524329.
975 Yeo, H., Yoon, Y., Madanat, S., 2013. Algorithms for bottom-up maintenance optimization for
976 heterogeneous infrastructure systems. Structure and Infrastructure Engineering, 9(4), 317-
977 328.
978 Zhang, L., Fu, L., Gu, W., Ouyang, Y., Hu, Y., 2017. A general iterative approach for the system-
979 level joint optimization of pavement maintenance, rehabilitation, and reconstruction planning.
980 Transportation Research Part B: Methodological, 105, 378-400.
981 Zhang, L., 2019. Optimal lifecycle management of transportation asset systems (Doctoral
982 dissertation. The Hong Kong Polytechnic University).
983